Afforestation impact on soil temperature in regional climate model simulations over Europe

Giannis Sofiadis[1], Eleni Katragkou[1], Edouard L. Davin[2], Diana Rechid[3], Nathalie de Noblet-Ducoudre[4], Marcus Breil[5], Rita M. Cardoso[6], Peter Hoffmann[3], Lisa Jach[7], Ronny Meier[2], Priscilla A.Mooney[8], Pedro M.M. Soares[6], Susanna Strada[9], Merja H. Töölle[10], Kirsten Warrach Sagi[7]

[1]Department of Meteorology and Climat-ology, School of Geology, Aristotle University of Thessaloniki, Thessaloniki, Greece
[2]Department of Environmental Systems Science, ETH Zurich, Zurich, Switzerland
[3] Climate Service Center Germany (GERICS), Helmholtz-Zentrum Hereon, Fischertwiete 1, 20095 Hamburg, Germany
Climate Service Centre Germany (GERICS), Helmholtz-Zentrum Geesthacht, Hamburg, Germany
[4]Laboratoire des Sciences du Climat et de l'Environnement; UMR CEA-CNRS-UVSQ, Université Paris-Saclay, Orme des Merisiers, bât 714, 91191 Gif-sur-Yvette CÉDEX, France.
[5]Institute of Meteorology and Climate Research, Karlsruche Institute of Technology, Karlsruche, Germany.
[6]Instituto Dom Luiz (IDL), Faculdade de Ciencias, Universidade de Lisboa, 1749-016 Lisboa, Portugal.
[7]Institute of Physics and Meteorology, University of Hohenheim, Stuttgart, Germany.
[8]NORCE Norwegian Research Centre AS/ Bjerknes Center for Climate Research, Bergen, Norway.
[9]International Center for Theoritical Physics (ICTP), Earth System Physics Section, Trieste, Italy.
[10]Universität Kassel, Center of Environmental Systems Research (CESR), Wilhelmshöher Allee 47, 34117 Kassel, Germany.

Correspondence to: Giannis Sofiadis (sofiadis@geo.auth.gr)

Abstract. In the context of the first phase of the Euro-CORDEX Flagship Plot Study (FPS) Land Use and Climate Across Scales (LUCAS), we investigate the afforestation biophysical impact of afforestation on the seasonal cycle of soil temperature over the European continent with an ensemble of ten regional climate models (RCMs). For this purpose, each ensemble member performed two idealized land cover experiments in which Europe is covered either by forests or grasslands. The multi-model mean exhibits a reduction of the annual amplitude of soil temperature (AAST) due to afforestation over all European regions, although this is not a robust feature among the models. In Mediterranean, the simulated AAST response to afforestation is between -4 K and +2 K while in Scandinavia the inter-model spread ranges from -7 K to +1 K. We then examine the role of changes in the annual amplitude of ground heat flux (AAGHF) and summer soil moisture content (SMC) in determining the effect of afforestation on AAST response. In contrast with the diverging results in AAST, all the models consistently indicate a widespread AAGHF decrease and summer SMC decline due to afforestation. The AAGHF changes effectively explain the largest part of the inter-model variance in AAST response in most regions, while the changes in summer SMC determine the sign of AAST response within a group of three simulations sharing the same land surface model. . In Mediterranean, the spread of simulated AAST response to afforestation is between -4 ºC to +2 ºC at 1 meter below the ground while in Scandinavia the inter-model spread ranges from -7 ºC to +1 ºC. We show that the large range in the simulated AAST response is due to the representation of the summertime climate processes and is largely explained by inter-model differences in leaf area index (LAI), surface albedo, cloud fraction and soil moisture, when all combined into a multiple linear regression. The changes in these drivers essentially determine the ratio between the increased radiative energy at surface (due to lower

albedo in forests) and the increased sum of turbulent heat fluxes (due to mixing-facilitating characteristics of forests), and consequently decide the changes in soil heating with afforestation in each model Finally, we pair FLUXNET sites to compare the simulated results with observation-based evidence of the impact of forest on soil temperature. In line with models, observations indicate a summer ground cooling in forested areas compared to open lands. The vast majority of models agree with the sign of the observed reduction in AAST, although with a large variation in the magnitude of changes. Overall, we aspire to emphasize the biophysical effects of afforestation on soil temperature profile with this study, given that changes in the seasonal cycle of soil temperature potentially perturb crucial biochemical processes. Robust knowledge on biophysical impacts of afforestation on soil conditions and its feedbacks on local and regional climate is needed in support ofto effective land-based climate mitigation and adapation policies. Such perturbations can be of societal relevance as afforestation is proposed as a climate change mitigation adaptation strategy.

1 Introduction

There is currently a strong policy focus on afforestation as aa possible greenhouse gases (GHG) mitigation strategy to meet ambitious climate targets (Grassi et al., 2017). The biogeochemical effects of afforestation or reforestation are mostly related to increased carbon stocks stored in vegetation and soil, as the total carbon stored in forests is nearly three times larger than carbon stored in croplands (Devaraju et al., 2015). However, understanding the full climate consequences of the large-scale deployment of such a strategy requires to consider also the biophysical effects of afforestation arising from changes in evapotranspiration efficiency, rooting depths and soil water holding capacity, surface roughness and surface albedo (Betts, 2000; Bonan, 2008; Davin and de Noblet-Ducoudre, 2010; Perugini et al., 2017; Duveiller et al., 2018).

Previous studies have attempted to quantify the biophysical impact of land-use changes (LUC) on global scale, employing either an ensemble of global climate earth system models (ESMGCMs) simulations (Pitman et al., 2009; Noblet-Ducoudré et al., 2012; Boisier et al., 2012; Lejeune et al., 2018) or applying a single ESMGCM individually (Claussen et al., 2001; Davin et al., 2007; Li et al., 2016). (Davin and de Noblet-Ducoudre, 2010) analysed an ESGCM's sensitivity to idealized global deforestation, indicating that the net biophysical impact results from the balance between radiative and non-radiative processes. In the same study,Over the tropical zone, deforestation induced a warming over the tropical zone owing to a reduction in evapotranspiration rate and surface roughness. . On contrary, deforestation resulted in whereas a deforestation-induced cooling simulated over the temperate- and boreal zones, because an albedo increase provided the dominant influence in these regions. In the context of Land-Use and Climate, IDentification of Robust Impacts (LUCID) model inter-comparison project, (Noblet-Ducoudré et al., 2012) diagnosed the LUC effects over North America and Eurasia between the present and the pre-industrial era. They found that deforestation caused a systematic surface albedo increase across all seasons, leading to a reduction in available energy accompanied by a decrease in the sum of turbulent fluxes. Furthermore, (Lejeune et al., 2018) using a suite of simulations from Coupled Model Inter-comparison Project Phase 5 (CMIP5) concluded that moderate deforestation over Eurasia and North America has substantially led to a local warming of present-day hot extremes since pre-industrial time.

Regional Climate Models (RCMs) constitute dynamical downscaling techniques applied over limited-area domains with boundary conditions either from global reanalysis or global climate model (GCM) output (Katragkou et al., 2015; Giorgi, 2019; Rummukainen, 2016). RCMs operate on higher resolutions than GCMs adding value~~e.g.~~ in regions with ~~variable~~complex orography and capturing exreme events (Soares et al., 2012; Cardoso et al., 2013; Warrach-Sagi et al., 2013). ~~Regional climate models (~~RCMs~~)~~ have been also used individually to address the LUC effects on regional scale (Gálos et al., 2013; Tölle et al., 2018; Cherubini et al., 2018; Belušić et al., 2019). ~~(~~Lejeune et al., 2015~~)~~ used a state-of-the-art RCM to explore the biophysical impacts of possible future deforestation on Amazonian climate. They demonstrated that the projected land cover changes for 2100 could slightly increase the mean annual surface temperature by 0.5 ºC and decrease the mean annual rainfall by -0.17 mm /day^{-1} compared to present conditions. Similar findings were demonstrated for a deforestation scenario over South-East Asia in ~~(~~Tölle et al., 2017~~)Tölle et al. 2017.~~ ~~(~~Strandberg and Kjellström, 2019~~)~~ performed regional climate simulations undertaking scenarios of maximum deforestation/reforestation over Europe using a single RCM. They concluded that total deforestation could result in a warmer summer by 0.5 ºC - 2.5 ºC in Europe, while the effect on precipitation was less certain. A more realistic land cover change study based on convection-permitting regional climate model simulations (Prein et al., 2015)~~(Prein et al. 2015)~~ suggested that increased cultivation of bioenergy crops by poplar trees can reduce future local maximum temperatures by up to 2 °C in central Europe (Tölle and Churiulin, 2021). ~~(Tölle et al. 2014).~~ ~~The crucial need to better constrain and represent the LUC biophysical forcing in regional climate simulations over Europe,~~ The crucial need for the assessment of LUC biophysical impacts on regional scale over Europe is addressed by the ~~, generated the Euro-CORDEX (Jacob et al., 2020) FPS~~ Land Use and Climate Across Scales (LUCAS) initiative (Rechid et al., 2017~~n.d.~~) which had been approved by WCRP CORDEX as a Flagship Pilot Study (FPS).~~which operates under the auspices of the World Climate Research Program (WCRP).)~~. It was initiated jointly by the European branch of the Coordinated Downscaling Experiments EURO-CORDEX (Jacob et al., 2014, 2020)~~(Jacob et al., 2014; 2020)~~ and the global model intercomparison study "Land-Use and Climate, IDentification of robust impacts" LUCID (Noblet-Ducoudré et al., 2012)~~(de Noblet-Ducoudré et al., 2012).~~ In the first phase of LUCAS, for the first time multi-model and multi-physics simulations were performed under a common experimental protocol to address the RCMs sensitivity to ~~extreme~~ idealized land use changes in Europe. The first experiment assumed a maximum forest coverage while the second a maximum grass coverage over Europe.

Contrasting these two idealized LUC experiments, ~~(~~Davin et al., 2020~~)~~ analysed the robustness of RCMs responses to afforestation and according to their results, afforestation implied an albedo-induced warming over northern Europe during winter and spring. Furthermore, the summer near-surface temperature response to afforestation was subject to large uncertainty, strongly related with disagreement among models in land-atmosphere interactions. Analysing a part of RCM ensemble established within LUCAS FPS, ~~(~~Breil et al., 2020~~)~~ examined the impact of afforestation on the diurnal temperature cycle in summer. Their results revealed that afforestation dampened the diurnal surface temperature cycle, while the opposite was true for the temperature in the lowest atmospheric model level. ~~The albedo parameterization in regional climate models could also play a role. Changing the albedo parameterization from a background to a vegetation type dependency reversed the~~

sign in the temperature signal (Tölle et al. 2018). Afforestation could also enhance snow melt and modify the land-atmosphere interactions in sub-polar and alpine climates through changes in snow-albedo effect in winter and spring (Mooney et al., 2021). The responses of atmospheric processes to afforestation have been extensively discussed in previous studies. However, the changes in soil temperature profile following the afforestation remain unexplored up to now in LUCAS community. (MacDougall and Beltrami, 2017) suggested that deforestation may has led to a long-term warming of the ground, associated with a reduction of heat fluxes towards the atmosphere. Here, we investigate the biophysical impact of afforestation on soil temperature across Europe from biophysical aspect, as simulated by a suite of ten RCMs established within the frame of the first phase of FPS LUCAS FPS. The comparison between two extreme LUC scenarios, representing the Europe entirely covered by forest and grass respectively, enable us to gain insights into the biophysical impacts of theoretical afforestation on soil temperature variations (Sect. 3.1). Taking into account the second heat conduction law, we examine both the annual amplitude of ground heat flux (AAGHF) (Sect. 3.2) and summer soil moisture content (SMC) (Sect. 3.3) responses to afforestation, in order to explain the inter-model spread in annual amplitude of soil temperature (AAST) (Sect. 3.4).). In order to explain the inter-model spread in annual amplitude of soil temperature (Sect. 3.4), we examine the changes in surface energy balance components with respect to differences in land-use parameters across RCMs (Sect. 3.2) and the response of soil moisture content to afforestation in summer (Sect. 3.3). In addition, we compare the simulated impact on AAST with observational evidence based on FLUXNET paired sites, classified as forest or open land (Sect. 3.5).

2 Data and Methods

2.1 Regional Climate Model ensemble

Two idealized LUC experiments are carried out using an ensemble of ten RCMs. **Table 1** provides a brief description of the RCM ensemble characteristics, while more information about the land and atmospheric setups can be found in (Davin et al., 2020) and in **Table S1** in the supplementary material. Compared to (Davin et al., 2020) the current model ensemble includes simulations from two additional RCMs (CCLM-CLM5.0 and WRFc-NoahMP) while one of the RCMs (RCA) is not included here because the necessary variables for the analysis were missing. Compared to CCLM-CLM4.5, CCLM-CLM5.0 is coupled with a modified version of CLM 5.0 (Lawrence et al., 2019) that includes biomass heat storage (Swenson et al., 2019; Meier et al., 2019). WRFc-NoahMP shares the same land component as WRFb-NoahMP but differs in the atmospheric set-up. Namely, WRFc-NoahMP used the Yonsei University (YSU) scheme (Hong et al., 2006) as planetary boundary layer (PBL) parameterization and MM5 as surface layer scheme, as opposed to MYNN Level 2.5 PBL (Nakanishi and Niino, 2009) in WRFb-NoahMP. In addition, new simulations were carried out for WRFb-NoahMP and WRFb-CLM4.0 to address minor bug fixes.

Table 1: Characteristics of the RCMs participating in the study. JLU – Justus-Liebig-Universität Gießen; BTU: Brandenburgische Technische Universität; KIT – Karlsruhe Institute of Technology; ETH – Eidgenössische Technische Hochschule Zürich; SMHI – Swedish Meteorological and Hydrological Institute; ICTP – International Centre for Theoretical Physics; GERICS – Climate Service Center Germany; IDL – Instituto Amaro Da Costa; UHOH – University of Hohenheim; BCCR – Bjerknes Center for Climate Research; AUTH – Aristotle University of

Formatted: Font: Bold

~~Thessaloniki. The full table including the parameterization schemes and settings used, can be found in (Davin et al., 2020).~~

~~Model name~~	~~Institute~~	~~RCM version~~	~~LSM~~	~~Soil column~~
~~CCLM-TERRA~~	~~JLU/BTU~~	~~COSMO_5.0_clm9~~	~~TERRA-ML~~	~~10 layers down to 15.3 m. First 9 (8) layers are thermally (hydrologically) active.~~
~~CCLM-VEG3D~~	~~KIT~~	~~COSMO_5.0_clm9~~	~~VEG3D (Breil et al., 2018)~~	~~10 layers down to 15 m. First 9 (8) layers are thermally (hydrologically) active.~~
~~CCLM-CLM4.5~~	~~ETH~~	~~COSMO_5.0_clm9~~	~~CLM4.5 (Oleson et al., 2013)~~	~~15 thermally active layers down to 42 m. The first 10 layers are hydrologically active.~~
~~CCLM-CLM5.0~~	~~ETH~~	~~COSMO_5.0_clm9~~	~~CLM5.0 (Lawrence et al., 2019)~~	~~25 thermally active layers down to 50 m. The first 20 layers are hydrologically active.~~
~~RegCM-CLM4.5~~	~~ICTP~~	~~RegCMv4.6.1~~	~~CLM4.5 (Oleson et al., 2013)~~	~~15 thermally active layers down to 42 m. The first 10 layers are hydrologically active.~~
~~REMO-iMOVE~~	~~GERICS~~	~~REMO2009~~	~~iMOVE (Wilhelm et al., 2014)~~	~~5 thermally active layers down to 9.8 m. One water bucket.~~
~~WRFa-NoahMP~~	~~IDL~~	~~WRFv3.8.1~~	~~NoahMP~~	~~4 layers down to 2 m.~~
~~WRFb-NoahMP~~	~~UHOH~~	~~WRFv3.8.1~~	~~NoahMP~~	~~4 layers down to 2 m.~~
~~WRFc-NoahMP~~	~~BCCR~~	~~WRFv3.8.1~~	~~NoahMP~~	~~4 layers down to 2 m.~~
~~WRFb-CLM4.0~~	~~AUTH~~	~~WRFv3.8.1~~	~~CLM4.0 (Oleson et al., 2010)~~	~~10 thermally and hydrologically active layers down to 3.43 m.~~

2.2 Experimental design

In LUCAS, each participating RCM undertook two different simulations, applying the same experimental design. In the first experiment, called FOREST, models are forced with a vegetation map representing a Europe fully covered by trees, where they can realistically grow. Bare lands~~, urban areas~~ and water bodies were conserved as in original model maps. In the second experiment, called GRASS, the models integrate the same vegetation map, with the only difference that trees are entirely replaced by grasslands. These maps are shown in **Figure S1** and ~~D~~detailed description about the creation of ~~these~~ maps and the way they are implemented into the respective RCMs can be found in ~~(~~Davin et al., 2020~~)~~. All simulations are performed over the Euro-CORDEX domain (Jacob et al., 2020) with a spatial resolution of 0.44º (~50 km), forced by ERA-Interim reanalysis data (Dee et al., 2011) at their lateral boundaries and at the lower boundary over sea. Our analysis covers the 30-year period 1986-2015 and focuses on the following eight European sub-regions as described in ~~(~~Christensen and Christensen, 2007~~)~~: Alps ~~(AL)~~, British Isles ~~(BI)~~, Eastern Europe ~~(EA)~~, France ~~(FR)~~, Iberian Peninsula ~~(IP)~~, Mediterranean ~~(MD)~~, Mid-Europe ~~(ME)~~ and Scandinavia ~~(SC)~~ (**Figure ~~S~~1**).

We consider the FORECAST minus GRASS differences, implying the impact of theoretical maximum afforestation on soil temperature in Europe. ~~The second heat conduction law~~ Fourier's second law of heat conduction is widely used by LSMs to update temperature in each soil layer (Eq. 1):

$$\frac{dT}{dt} = \frac{d}{dz}[k * \frac{dT}{dz}] \quad \frac{\partial T}{\partial t} = \frac{\partial}{\partial z}[k * \frac{\partial T}{\partial z}]$$

~~where k is thermal diffusivity ($m^2 s^{-1}$) defined at the layer node depth z (m), t is time (s) and $\frac{dT}{dz}$ is the spatial gradient of temperature (K m^{-1}) in the vertical direction z (m).~~

~~The spatial gradient of soil temperature is strongly linked with the ground heat flux (GHF) quantity, while the thermal diffusivity is a function of soil texture and moisture. Since soil texture remains unchanged in our experiments, soil moisture is the only variable which influence the thermal diffusivity. Particularly, changes in soil moisture alter the heat capacity of soil column and consequently affect the soil temperature variations. In the present analysis, GHF is calculated as the residual of surface energy balance because the actual GHF outputs were not available in most models. A main caveat of this approach constitutes the fact that when the soil is decoupled from the upper atmospheric boundary layer (eg snow covered ground), the residual of surface energy balance does not represent the energy exchange on soil surface but the energy budget on the atmosphere-snow interface.~~

where $\frac{\partial T}{\partial t}$ is the time rate of soil temperature (K s^{-1}) and $\frac{dT}{dz}$ is the spatial gradient of soil temperature (K m^{-1}) in the vertical direction z (m). The quantity k represents the thermal diffusivity ($m^2 s^{-1}$) defined at the layer node depth z(m) and is equal to the ratio of thermal conductivity to volumetric heat capacity (p ~~*x~~ c_m, where p is mass density and c_m specific heat capacity per unit mass). In RCMs, k is time dependent~~variable~~ and is parameterized depending on soil type and composition (mineral components, organic matter content), on bulk density and soil wetness. In our experiments, soil texture remains unchanged and RCMs do not account for possible occurrence of heat sources or sinks (such as organic matter or carbon decomposition) in the realm where soil heat flow takes place. Thus, the potential changes in soil wetness with afforestation constitute the main driver of differences in soil thermal diffusivity in our experiments. In this way, we use soil moisture response to afforestation as a potentially explanatory variable of soil temperature variations in RCMs.

Similar to (Breil et al., 2020), we employ the residual of energy balance at land surface in order to express the surface energy input into the ground. Specifically, we define as energy input into ground the residual energy amount resulting from available radiative energy (net shortwave + incoming longwave radiation) minus the sum of turbulent heat fluxes (latent and sensible heat flux), without accounting for likely deviation of surface energy budget from assumed balance in models (Constantinidou et al., 2020b). Our analysis on the changes of surface energy balance components due to afforestation is carried out for summer season, when models disagree both on the sign and magnitude of soil temperature response. Thus, the land surface is assumed to be snow-free. Also, the current RCMs do not account for heat storage into biomass over land surface, apart from CCLM-CLM5.0. A detailed description on the structure of land-atmosphere exchange in the different LSMs is provided in (Breil et al., 2020).

Formatted: Font: Not Bold
Formatted: Font: 12 pt
Formatted: Font: 12 pt
Formatted: Font: Not Bold
Formatted: Font: 12 pt
Formatted: Font: 12 pt
Formatted: Font: Not Bold
Formatted: Font: Not Bold
Formatted: Font: Not Bold
Formatted: Font: Not Bold
Formatted: Font: Not Bold
Formatted: Font: Not Bold
Formatted: Font: Not Bold
Formatted: Font: Not Bold

2.3 FLUXNET observational data

We use measured or high-quality gap-filled data of soil temperature on monthly scale from the FLUXNET2015 Tier 2 dataset to complement the model-based analysis. Detailed documentation on data and processing methods can be found in ~~(~~Pastorello et al., 2020~~)~~.

In order to extract the potential effect of afforestation from observations, we employ a space-for-time analogy by searching for pairs of neighbouring flux towers located in~~over~~ forest (deciduous, evergreen or mixed trees) and open land (grasslands or croplands), respectively. This approach has been used in previous studies aiming to investigate biophysical impacts of local LUC and evaluate LSM performance (Broucke et al., 2015; Chen et al., 2018). In search for site pairs, the following criteria were defined: the two sites have to 1) be located in the Euro-CORDEX domain, 2) differ in the type of vegetation, one site being forested and the other one being either cropland or grassland, 3) have a linear distance within the horizontal resolution of the performed simulations (less than 50 km), 4) have a common measurement period of at least two years, and 5) provide measurements at common depth below the ground surface. In total, we found 14 sites that met our criteria and combined in ten pairs. Their locations are depicted in **Figure 1** and their characteristics are reported in **Table 2**. The median linear distance between the paired sites is 11.4 km and their median elevation difference is 125 m.

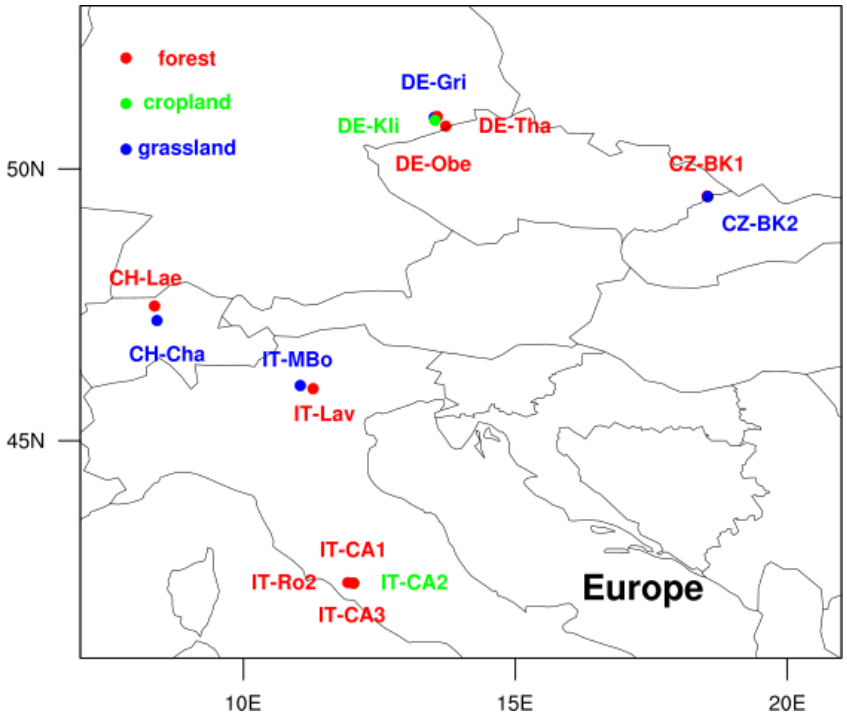

~~Figure 1: Location of the sites selected from FLUXNET2015 dataset.~~

~~Table 2: Characteristics of the sites selected from FLUXNET2015 dataset. DBF – Deciduous Broadleaf Forest; ENF – Evergreen Needleleaf Forest; MF – Mixed Forest; CRO – cropland; GRA – grassland, as described by the International Geosphere-Biosphere Programme (IGBP) classification scheme.~~

~~Pair ID~~	~~FLUXNET site ID~~	~~(Latitude, Longitude)~~	~~Elevation (m)~~	~~Land cover type~~	~~Distance (km)~~	~~Time period~~	~~Measurement depth~~
~~1~~	~~IT-CA1~~	~~(42.380,12.026)~~	~~200~~	~~DBF~~	~~0.3~~	~~2011-2014~~	~~15cm~~
	~~IT-CA2~~	~~(42.377,12.026)~~	~~200~~	~~CRO~~			
~~2~~	~~IT-CA3~~	~~(42.380,12.022)~~	~~197~~	~~DBF~~	~~0.4~~	~~2011-2014~~	~~15cm~~
	~~IT-CA2~~	~~(42.377,12.026)~~	~~200~~	~~CRO~~			
~~3~~	~~IT-Ro2~~	~~(42.390,11.920)~~	~~160~~	~~DBF~~	~~8.7~~	~~2011-2012~~	~~15cm~~
	~~IT-CA2~~	~~(42.377,12.026)~~	~~200~~	~~CRO~~			

4	CZ-BK1	(49.502,18.536)	875	ENF	0.9	2004-2012	5cm
	CZ-BK2	(49.494,18.542)	855	GRA			
5	DE-Tha	(50.962,13.565)	385	ENF	4.1	2004-2014	10cm
	DE-Gri	(50.950,13.512)	385	GRA			
6	DE-Obe	(50.786,13.721)	734	ENF	23.4	2008-2014	10cm
	DE-Gri	(50.950,13.512)	385	GRA			
7	DE-Tha	(50.962,13.565)	385	ENF	8.4	2004-2014	10cm
	DE-Kli	(50.893,13.522)	478	CRO			
8	DE-Obe	(50.786,13.721)	734	ENF	18.4	2008-2014	10cm
	DE-Kli	(50.893,13.522)	478	CRO			
9	IT-Lav	(45.956,11.281)	1353	ENF	19.3	2003-2013	10cm
	IT-Mbo	(46.014,11.045)	1550	GRA			
10	CH-Lae	(47.478,8.364)	689	MF	30	2005-2014	10cm
	CH-Cha	(47.210,8.41)	393	GRA			

The close proximity between the flux towers of paired sites ensures almost similar atmospheric conditions, so that differences can be primarily attributed to the different vegetation cover. Applying a simple linear correlation test, the differences either in elevation or separation between the flux towers of paired sites are not the dominant factors in determining the changes in AAST ($r = -0.2$ and $r = -0.3$, respectively).

For comparison with the RCMs, we consider the observed mean monthly soil temperature differences (forest minus open land) averaged over all paired sites. This is then compared with the mean of the grid cells matching the locations of the observational pairs in the various RCMs (FOREST minus GRASS). Modelled soil temperature was linearly interpolated to the common measurement depth that is available for each pair site and averaged over the time period 2003-2014 which covers the observational time span.

Last but not least, the observational setup does not fully resemble the experimental design applied in RCM ensemble. The spatial scale of afforestation applied in models is significantly different from the small forest patches the flux towers are located in. The extreme afforestation in RCMs has the potential to triggers atmospheric feedbacks which strongly modify the local and regional climate, whereas such feedbacks are not realistic in observations. The theoretical maximum afforestation in RCMs has the potential to induce changes in large-scale atmospheric circulation, which can create tele-connections (Swann et al., 2012) that modify the regional cloud cover (Laguë and Swann, 2016) and thus the regional climate conditions. Such feedbacks are not realistic in observations, where most forest measurement locations are located in relatively small forest patches surrounded by open land and is almost unlikely to alter the climate conditions on regional scale.

3. Results

3.1 Soil temperature response

The afforestation (FOREST minus GRASS) effect on the annual amplitude of soil temperature (AAST) at 1 meter below the ground surface is shown in **Figure 2** ~~**2** shows the afforestation (FOREST minus GRASS) effect on the annual amplitude of soil temperature (AAST) at 1 meter below the ground surface~~. Similar figures can be found for temperature at soil depths of 2 cm, 20 cm and 50 cm in the supplementary material (**Figures S2, S3, S4**) AAST is calculated as the difference between the warmest and the coldest month of an average year (based on the 1986-2015 climatology), implying that the maximum and minimum value may occur in different months depending on regions.

A large range of AAST response is simulated across RCMs. ~~Six out of the ten simulations show a decrease in the AAST due to afforestation in most regions (**Figure S2**)~~. The sign of differences in AAST does not change with depth in almost all models across regions (**Figure S5**). Within the ensemble, the magnitude of AAST response at 1 meter below the ground varies across regions from -7.1 ºC to 1.8 ºC. Six out of the ten simulations show a decrease in the AAST due to afforestation in most regions .Four out of these six ensemble members employ a version (4.0, 4.5 and 5.0) of the CLM land surface model (LSM), coupled with a different atmospheric model (CCLM, RegCM or WRF). Therefore, it can be assumed that~~,~~ the agreement in sign of changes between these simulations resides to a great extent in the choice of a similar LSM. Also, the latter finding holds true for three out of ten ensemble members exhibiting the opposite behaviour, namely an increase in AAST mostly at deeper soils over southern and eastern Europe. These three members utilize the NoahMP LSM coupled to different WRF atmospheric model configurations (WRFa, WRFb and WRFc); WRFa shows the most intense and systematic changes in AAST with afforestation (close to 2 ºC ~~K~~ in several regions), while the other two configurations (WRFb and WRFc) show absolute changes less than 1 ºC ~~K~~ at all soil depths. ~~The weakest response is simulated by REMO-iMOVE with temperature changes ranging from -0.5 K in southern Europe to +0.5 K in Scandinavia.~~ Last, WRFb-CLM4.0 and REMO-iMOVE exhibit similar responses with temperature changes ranging from -1 ºC in southern Europe to +0.5 ºC in Scandinavia.

It is worth noting that the differences between simulations with the same atmospheric model (WRFb) coupled to different LSMs (NoahMP and CLM) disagree in sign of changes, especially over southern Europe. This finding suggests again that the choice of the LSM drives in a great extent the sign of changes in AAST (increase/decrease), while the choice of the atmospheric model further modulates (dampens/enhances) the magnitude of the signal. Another sub-ensemble is built around the CCLM atmospheric model participating with three different LSMs (TERRA, VEG3D, CLM version 4.5 and 5.0) illustrating diverse results; CCLM-TERRA exhibits the strongest decrease in AAST with maximum changes exceeding -4 ºC ~~K~~ over many regions. The CCLM-CLM configurations provide similar responses with maximum changes up to -2 ºC ~~K~~. The CCLM-VEG3D exhibits a distinct behaviour with small AAST increases over central Europe and large AAST decrease of more than -5 ºC in northern Europe~~.~~

Formatted: Font: Not Bold

Formatted: English (United States)

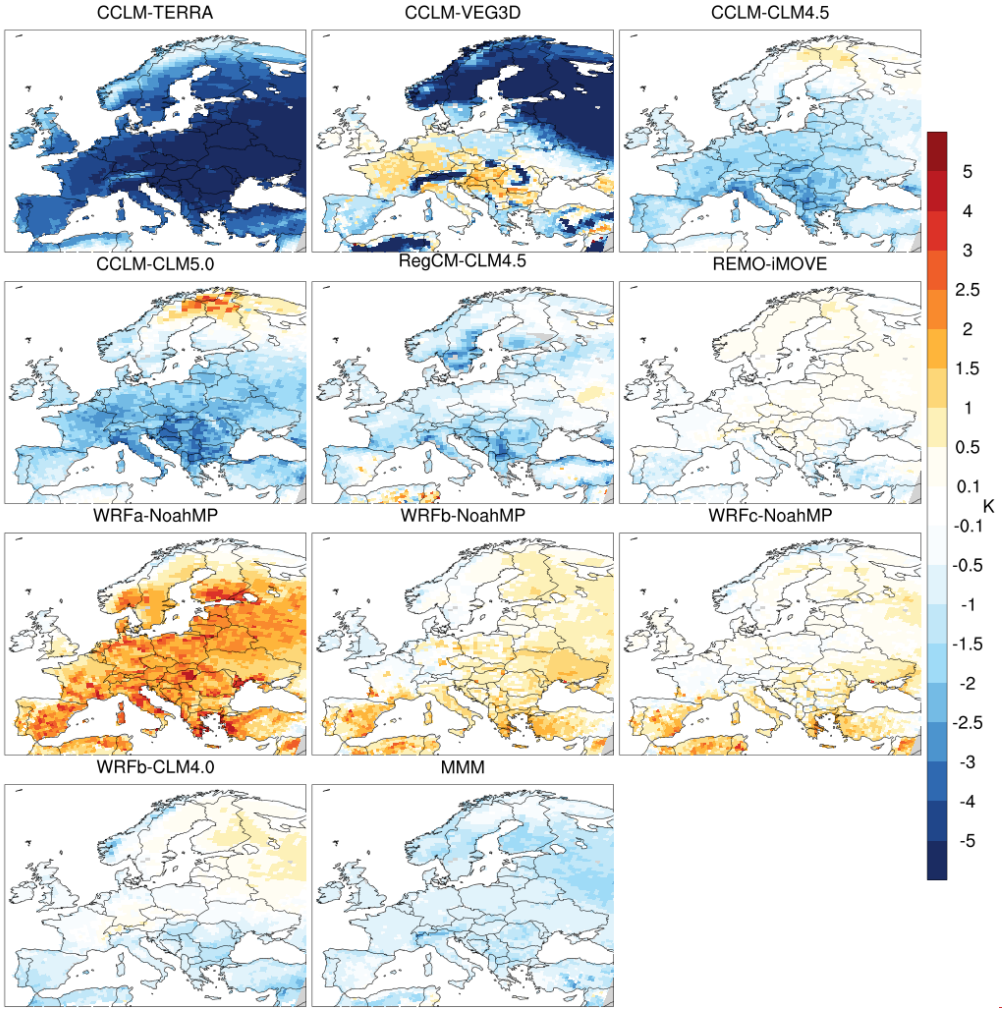

~~Figure 2: Afforestation (FOREST minus GRASS) impact on the annual amplitude of soil temperature (AAST) at 1 meter depth. MMM: Multi-Model-Mean.~~

To better understand the changes in AAST, we examine the ~~annual cycles of soil temperature for both experiments, FOREST (red) and GRASS (blue)~~afforestation effect (FOREST minus GRASS) on mean monthly temperature at 2 cm, 20 cm , 50 cm,

and 1 meter below the ground over two European sub-regions, the Mediterranean (**Figure 3**) and Scandinavia (**Figure 4**). These two regions are selected as they are representative of southern and northern Europe, respectively, while similar figures can be found for all European subregions in the supplementary material (**Figures S63-S118**). ~~Moreover, in **Figures S9-S16** we present the afforestation effect on mean monthly soil temperature within the top 1 meter of the soil over all the regions for each modelling system.~~

Over the Mediterranean region almost all models respond to afforestation, with REMO-iMOVE exhibiting ~~the lowest sensitivity to the land cover change forcing in all seasons~~ an almost constant temperature increase of small magnitude at all soil depths and seasons. From the remaining simulations, six out of the nine show that summer (maximum) soil temperatures are higher in the GRASS than in the FOREST experiment. All simulations included in this category involve the CLM (coupled with CCLM, RegCM, WRF), TERRA and the VEG3D LSMs. The winter (minimum) soil temperatures in the same modelling systems ~~do not differ for the two experiments (FOREST and GRASS)~~ are not considerably affected by afforestation and thus we can attribute the decrease in AAST, discussed before, exclusively to the summertime climate processes over the Mediterranean region. From t~~T~~he ~~three~~ remaining simulations of the ensemble ~~show the opposite behaviour~~, WRFa-NoahMP and WRFb-NoahMP show the opposite behaviour with higher forest soil temperatures in summer, while the temperature response in WRFc-NoahMP is small and mixed across months. ~~and they all involve the NoahMP LSM~~. Similar to the first group of simulations, the winter soil temperature sensitivity to afforestation is pretty small, and as a result the AAST in WRFa-NoahMP and WRFb-NoahMP modelling systems has a positive sign of change.

In Scandinavia, ~~considerable disagreement in the model behaviours is visible, as three members show a clear decrease in summer soil temperature similar to the Mediterranean area (CCLM-TERRA, CCLM-VEG3D, RegCM-CLM4.5), two models exhibit the opposite behaviour with increased soil temperature (CCLM-CLM5.0, WRFa-NoahMP) and the rest modelling systems appear not to be sensitive to afforestation across the seasons. Obviously, the response of the modelling systems is mostly based on the selection of the LSM; the CCLM model coupled to TERRA, VEG3D and CLM provides totally different results, with the CCLM-VEG3D being the most responsive (up to -7 K) to afforestation during the summer. In winter, the soil temperature differences due to afforestation are small and with a tendency for increase. As seen in **Figure 4**, the simulated response exhibits great variability during the summer season, when models disagree both on the sign and magnitude of changes~~ a large spread in soil temperature response is simulated across RCMs in summer. REMO-iMOVE together with WRF modelling systems exhibit a small constant warming in almost all seasons and soil depths, with WRFa-NoahMP showing the most intense warming of 1.5 ^{o}C in summer. The response of the rest modelling systems is mostly based on the selection of the land component, since the CCLM model coupled to TERRA, VEG3D and CLM provides largely different results. CCLM-TERRA and CCLM-VEG3D show a temperature decrease at all soil depths, with CCLM-VEG3D being the most responsive with changes up to -9 ^{o}C in uppermost soil layer. CCLM-CLM4.5 exhibits small sensitivity across seasons with a tendency for temperature decrease in summer (similar response from RegCM-CLM4.5), while in CCLM-CLM5.0 the sign of changes switches from negative in upper layers to positive in deeper layers. In winter, the soil temperature differences due to afforestation are small in the majority of simulations and with a tendency for an increase.~~.~~

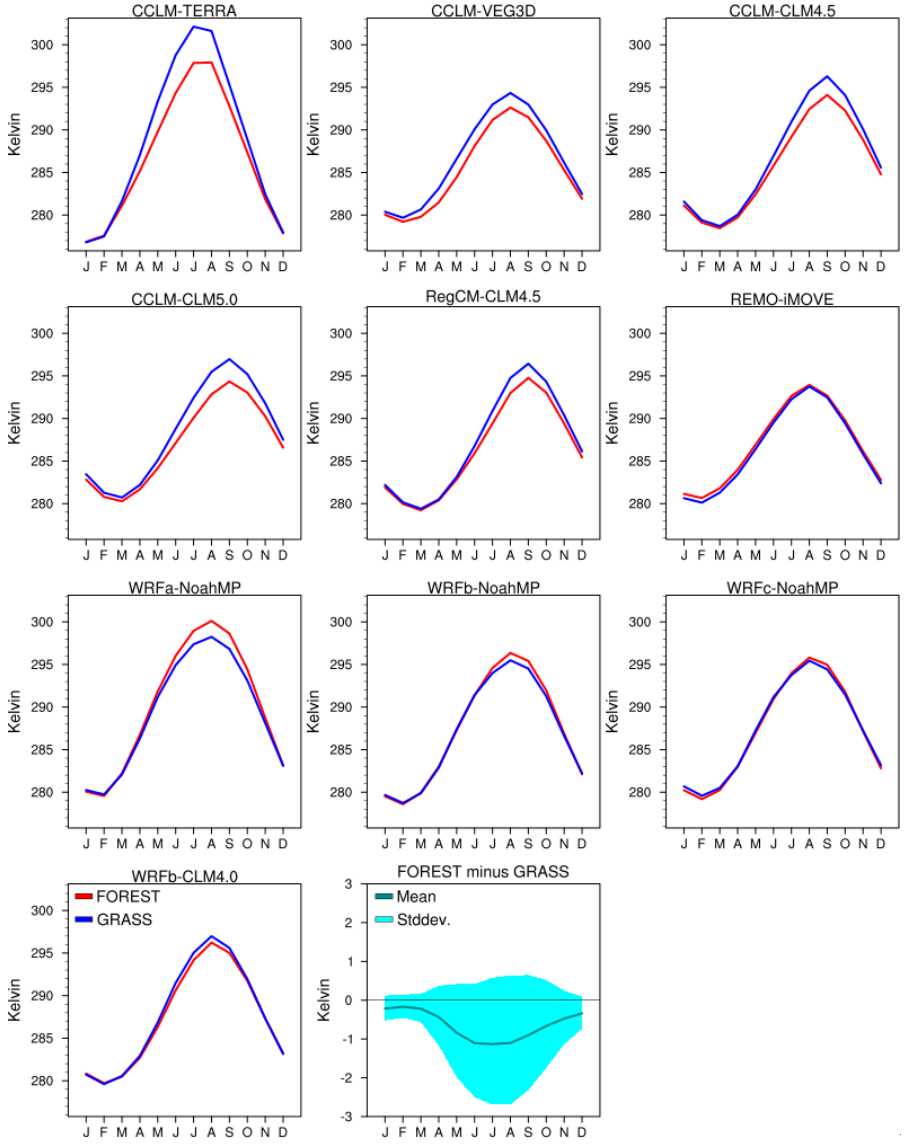

Figure 3: Annual soil temperature cycle for FOREST and GRASS over Mediterranean.

Formatted: Don't keep with next

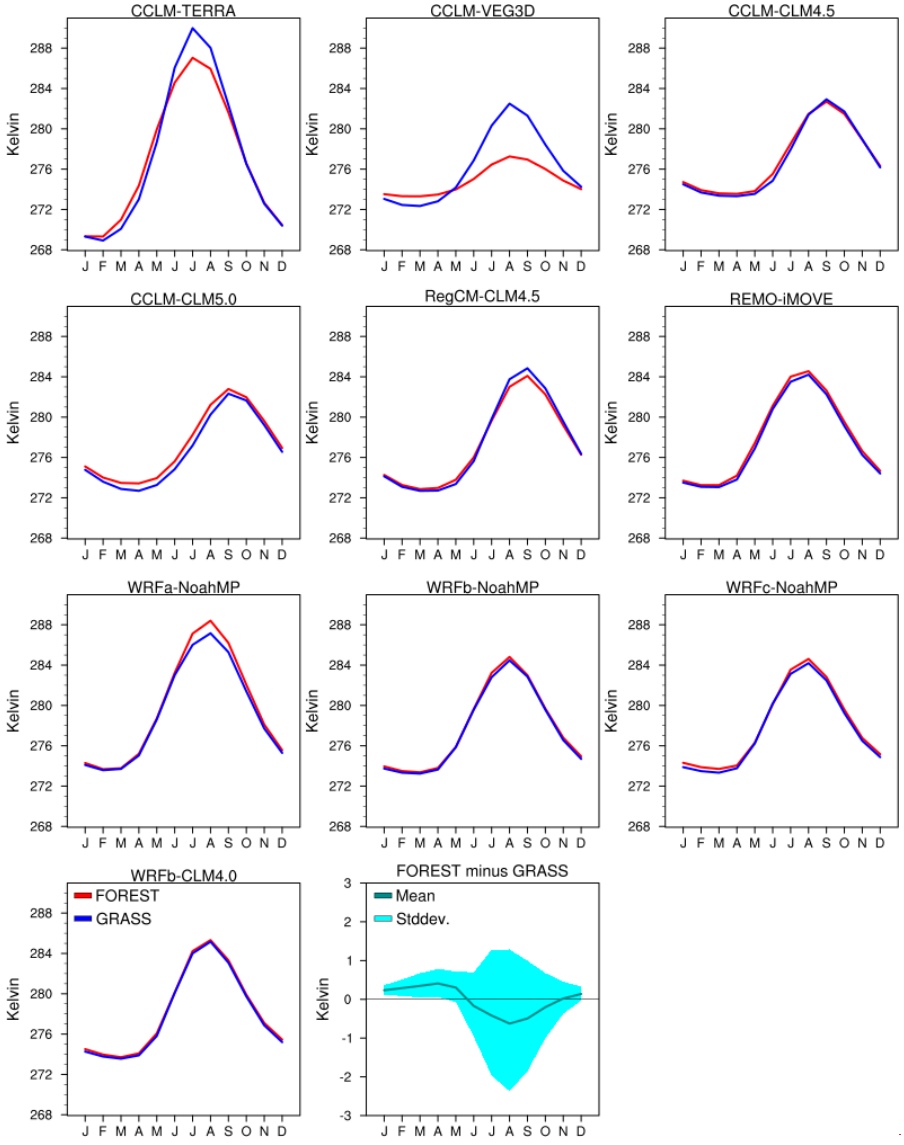

Figure 4: Annual soil temperature cycle for FOREST and GRASS over Scandinavia.

~~3.2 Annual amplitude of GHF~~ 3.2 Surface energy ~~input~~availability

~~In this section, we focus on the annual amplitude of GHF (AAGHF) as a potential driver for the AAST response to afforestation. Taking into account the second heat conduction law, a larger (smaller) AAGHF could result in a larger (smaller) AAST, when considering equal soil moisture conditions between the two experiments.~~

As reported in previous section, the simulated AAST response exhibits great variability during the summer season, when models disagree both on the sign and magnitude of changes. For this reason, it is essential to examine the changes in the available energy to warm the ground across RCMs in summer.

Figure 5 shows maps of the afforestation impact on the surface energy input into the ground in summer or the residual of surface energy balance, as defined in Section 2.2. The pattern of changes is largely heterogeneous between the models and correlates well with the spatial pattern of changes in AAST. The choice of LSM affects the magnitude of changes; different scales of decrease are seen between the members sharing the CCLM atmospheric model, especially between CCLM-VEG3D and CCLM-TERRA in central Europe. CCLM-CLM4.5 and CCLM-CLM5.0 provide similar responses with larger changes in southern Europe (close to -10 W/m^{-2}). Furthermore, the choice of LSM drives the sign of changes over southern Europe between WRFb-NoahMP and WRFb-CLM4.0. The contribution of atmospheric component is mostly related to the magnitude of changes; between RegCM-CLM4.5 and CCLM-CLM4.5, the latter provides stronger response in southern and central Europe, while between WRF-NoahMP modelling systems, WRFa-NoahMP stands out for its intense increase in surface energy input of more than 10 W/m^{-2} in several regions.

~~**Figure 5** shows maps of the afforestation impact on the AAGHF in Europe. In contrast to the diverse simulated response in AAST, all the ensemble members consistently show a reduction in AAGHF due to afforestation in all European subregions (**Figure S17**). Scandinavia appears to be the most sensitive among the regions, where four out of the ten ensemble members show a reduction in AAGHF greater than -10 W/m^2. The WRF-NoahMP modelling systems together with REMO-iMOVE show small AAGHF changes compared to the rest of the models, especially over the central and southern Europe. The choice of LSM affects the magnitude of changes in AAGHF; different scales of AAGHF decrease are observed between the members sharing the CCLM atmospheric model, especially between CCLM-VEG3D and CCLM-TERRA. Also, in central Europe several grid-cells in CCLM-VEG3D exhibit the opposite behaviour, namely a small AAGHF increase.~~

Formatted: Font: Bold

Formatted: Superscript

Formatted: English (United States)

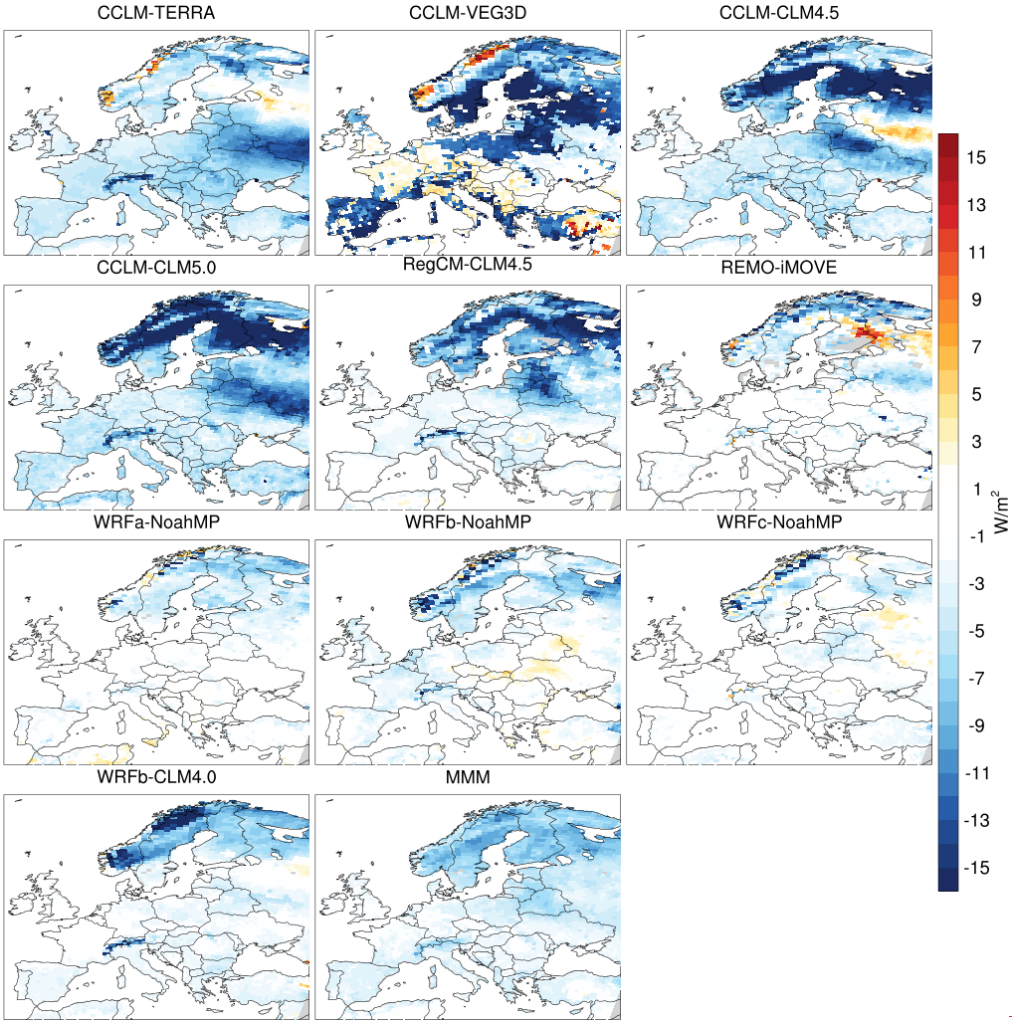

320 **~~Figure 5: Afforestation (FOREST minus GRASS) impact on annual amplitude of ground heat flux (AAGHF). MMM:Multi-Model-Mean.~~**

~~To further understand the AAGHF response, we examine the annual GHF cycles for both experiments, FOREST (red) and GRASS (blue) over the Mediterranean (**Figure 6**) and Scandinavia (**Figure 7**). Similar figures can be found for the rest~~

~~European subregions in the supplementary material (**Figure S18-S23**).~~ The heterogeneity in the changes of surface energy availability with afforestation is largely consistent with the disagreement in the changes of AAST among RCMs. Thus, it is crucial to explore the origin of large inter-model spread in changes of surface energy balance in summer. Below, we examine the afforestation impact on the different components of surface energy balance for each RCM over Mediterranean (**Figure 6**) and Scandinavia (**Figure 7**). Similar figures can be found for the rest European sub-regions in the supplementary material (**Figures S12-S17**). The analysis of differences in surface energy balance components is performed with respect to changes in land-use characteristics in each RCM, such as leaf area index (LAI), surface roughness and surface albedo. Positive (negative) values indicate an increase (decrease) due to afforestation.

In both regions, all ~~the~~ models (except from CCLM-TERRA) consistently show an increase in net shortwave radiation at the surface due to afforestation, which is a result of lower albedo in FOREST compared to GRASS experiment ~~(Figure ???)~~. The changes vary across RCMs from -5 W~~/~~m^{-2} to 25 W~~/~~m^{-2} over Mediterranean and from -15 W~~/~~m^{-2} to 35 W~~/~~m^{-2} over Scandinavia. In Scandinavia, the changes in net shortwave radiation are stronger than Mediterranean. This is attributed to the fact that the forests in Scandinavia consist of needleleaf trees, which have lower albedo values compared to broadleaf trees dominating in the rest regions of Europe. Furthermore, the WRF configurations exhibit more pronounced increases in net shortwave radiation with respect to other RCMs, which is linked to stronger reductions in albedo values in these simulations (**Figure 6f**, **Figure 7f**). Moreover, the albedo effect is further intensified by a reduction in cloud fraction with afforestation over Scandinavia in WRF configurations (**Figure 7c**). In CCLM-TERRA, the reduced net shortwave radiation is due to a pronounced increase in cloud fraction with afforestation triggered by a strong and widespread increase in evaporation rates (Davin et al., 2020). Cloud fraction is also increased with afforestation in other CCLM members, however the reduced incoming shortwave radiation is offset by the albedo effect and thus the changes in net shortwave radiation have positive sign in these simulations.

The increase in available radiative energy at the surface with afforestation is followed by an increase in sensible heat flux, which is another robust feature among simulations. According to ~~(~~Breil et al., 2020~~)~~, the increase in sensible heat flux with afforestation is attributed to higher surface roughness values in forests compared to grasslands. Generally, the high surface roughness values favour the mixing of atmosphere and enhance the heat exchange between the surface and the upper air. In the current model ensemble, the changes in sensible heat vary across RCMs from +5 W~~/~~m^{-2} to +26 W~~/~~m^{-2} over Mediterranean and from -16 W~~/~~m^{-2} to +35 W~~/~~m^{-2} over Scandinavia. Again, the only RCM which exhibits a reduction in sensible heat flux is CCLM-TERRA over Scandinavia, because of the pronounced increase in latent heat with afforestation. Moreover, WRF configurations exhibit the strongest changes in sensible heat flux within ensemble, especially over Scandinavia. As previously shown, afforestation induced intense increase in net shortwave radiation in these simulations, owing to strong reductions in albedo in combination with decreases in cloud fraction. Thus, a larger part of radiative energy is available to be transformed into sensible heat flux in these simulations. At the same time, the high surface roughness of needleleaf trees dominating in Scandinavia facilitate the energy exchange between ground and atmosphere in the form of turbulent heat fluxes.

While RCMs consistently show an increase in sensible heat flux, the agreement is much lower for the response of latent heat flux to afforestation. In Scandinavia, a tendency for increase in latent heat is noted, but in Mediterranean the simulated response

Formatted: Font: Bold

Formatted: Font: Bold

Formatted: Font: Bold

Formatted: Font: Bold

is mixed. In general, the sum of turbulent heat fluxes is increased with afforestation in all models and it's largely attributed to intense and widespread increase in sensible heat flux.

To sum up, all RCMs respond to afforestation in the same way. That is, afforestation leads to increased available radiative energy at the surface due to lower albedo values in FOREST experiment compared to GRASS. In parallel, a large part of this additional radiative energy is transformed into turbulent heat energy due to the mixing-facilitating forest characteristics, such as the high LAI and roughness values, which enhance the heat exchange between the ground and upper atmosphere. The balance between the increased available radiative energy and the increased sum of turbulent heat fluxes will determine if the surface energy input into the soil will be increased or decreased with afforestation in each RCM. Since these processes are differently weighted in each modelling system depending on land-use characteristics, the resulting energy input into the soil varies within the model ensemble in terms of the sign and magnitude of changes. In CCLM-TERRA, CCLM-VEG3D, CCLM-CLM4.5, CCLM-CLM5.0 and RegCM-CLM4.5 the soil heating is decreased with afforestation in summer over Mediterranean and Scandinavia, because the increased available radiative energy is compensated by the increased sum of turbulent heat fluxes. On the other hand, REMO-iMOVE and the sub-ensemble built around NoahMP exhibit an increase in soil heating with afforestation, since the increase in the sum of turbulent heat fluxes is not enough to compensate their pronounced increase in net shortwave radiation.

~~Over the Mediterranean region, RegCM-CLM4.5 together with the sub-ensemble around the CCLM model show seasonal contrasts in the GHF response to afforestation. Specifically, larger GHF values are found for GRASS during the spring and summer seasons, whereas the GHF is larger for FOREST during the autumn and winter seasons. The switch from NoahMP to CLM4.0 in WRFb atmospheric configuration alters the pattern of GHF changes; WRFb-NoahMP shows low sensitivity to afforestation with small increase during the summer, while WRFb-CLM4.0 exhibits a GHF decrease during the warm months. The remaining modelling systems show minor GHF changes throughout the year.~~

~~Over Scandinavia, all RCMs except WRF-NoahMP modelling systems, present seasonal contrasts in GHF changes similar to Mediterranean area; larger GHF values for GRASS during summer, but larger GHF for FOREST during autumn, winter and spring. The dampening of the annual GHF cycle over Scandinavia is a robust feature among the models, although is not reflected in the mixed AAST response, where the models produce a large spread in summer soil temperature due to afforestation as reported in previous section.~~

~~The GHF in WRF-NoahMP modelling systems exhibits low sensitivity to afforestation in both regions. The small decrease in AAGHF, originated from small GHF differences during spring, is not consistent with the AAST increase in these simulations. Thus, the changes in AAGHF could not be considered responsible for the AAST response in simulations with NoahMP.~~

Formatted: English (United States)

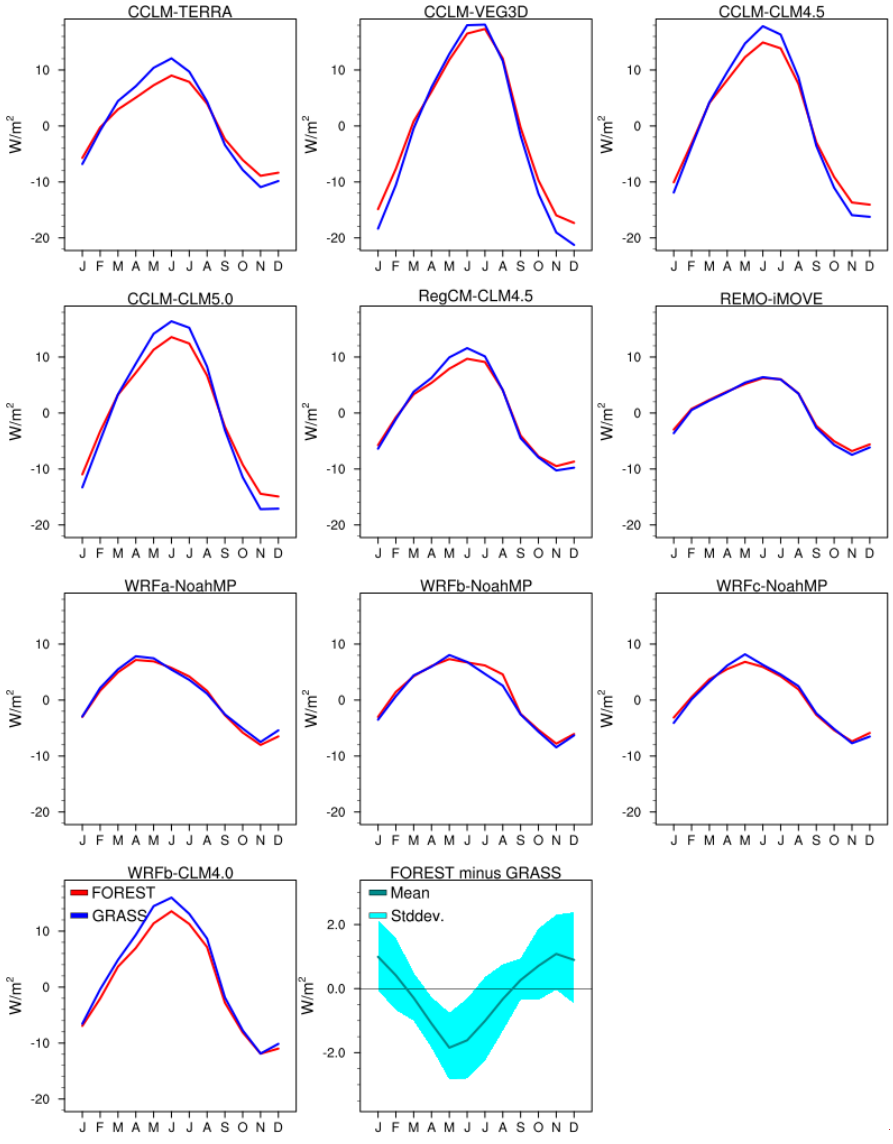

~~Figure 6: Annual GHF cycle for FOREST and GRASS over Mediterranean.~~

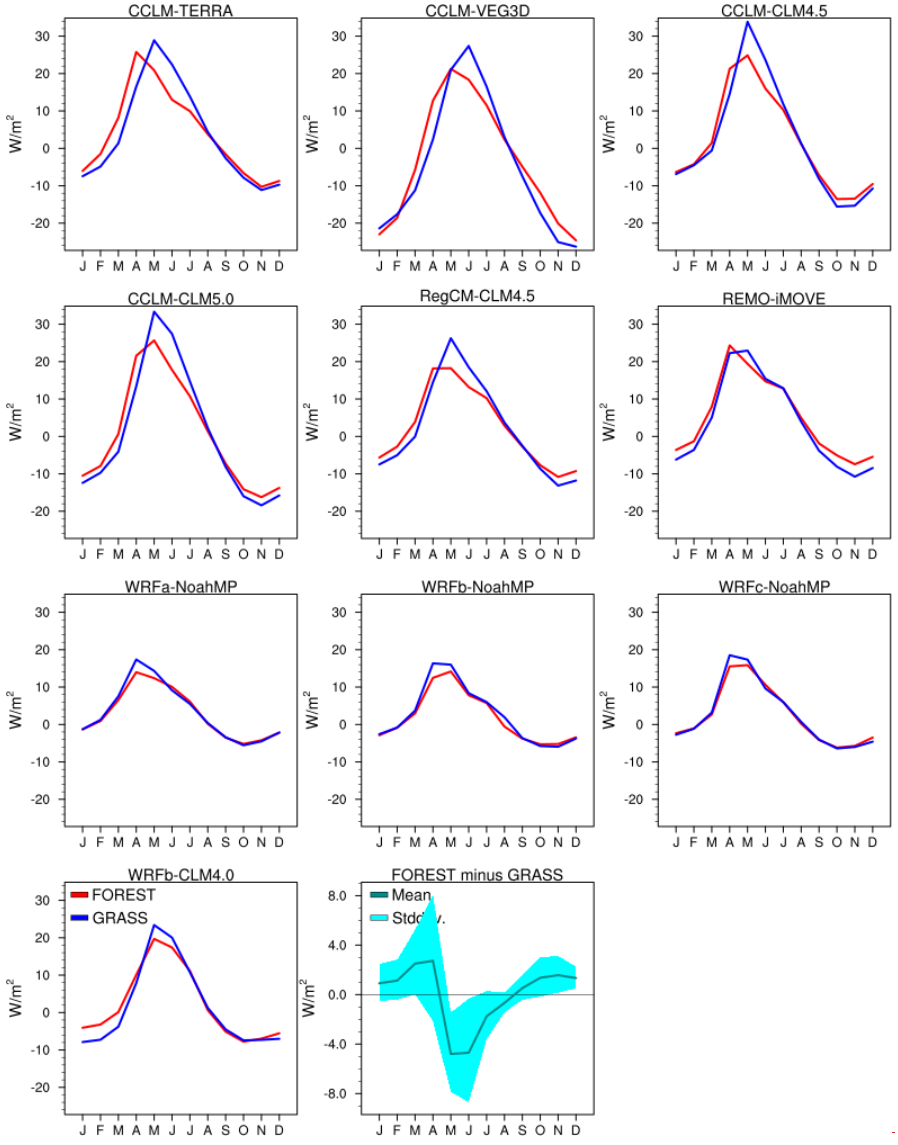

~~Figure 7: Annual GHF cycle for FOREST and GRASS over Scandinavia.~~

In **Figure 8** and **Figure 9** we show the year-round changes in surface fluxes over Mediterranean and Scandinavia regions, in order to discuss the underlying processes behind the dampening of the annual GHF cycle with afforestation. Similar figures can be found for the rest European subregions in the supplementary material (**Figures S24-S29**).

Over both regions, all the ensemble members exhibit a widespread increase in net radiation during the autumn and winter, which is a direct consequence of the decreased surface albedo with afforestation. This increase in net radiation leads to larger GHF values with afforestation during these seasons. In spring and summer, the increase in net radiation is even more pronounced since the incoming solar radiation becomes greater over the northern hemisphere during these seasons. Especially over Scandinavia during spring, the net radiation is sharply increased because of the snow masking effect of trees. However, the increased available radiative energy with afforestation is accompanied by a systematic increase in the sum of turbulent fluxes. This is attributed to high surface roughness which characterize the forested areas and enhance the heat exchange in soil-vegetation-atmosphere continuum (Breil et al., 2020). In most simulations the afforestation-induced increase in the sum of turbulent fluxes overcompensate the radiative energy gain during the warm months. Thus, GHF is smaller with afforestation during spring and summer over the Mediterranean region. For Scandinavia, this holds true only for summer, since the enhanced turbulent heat fluxes are not strong enough to offset the large increase in net radiation during spring. The seasonal pattern of GHF changes is not reproduced by REMO-iMOVE over Mediterranean and the sub-ensemble around NoahMP. REMO-iMOVE shows small changes in surface fluxes which is probably attributed to the low albedo sensitivity to afforestation across the seasons in its simulations. The modelling systems with NoahMP exhibit strong increase in net radiation especially during summer, may related to the reduced cloud cover with afforestation in these simulations (Breil et al., 2020). The seasonal contrast in GHF changes is not illustrated in WRF-NoahMP modelling systems, since the enhanced heat fluxes are almost equal with the increased radiative energy in most months.

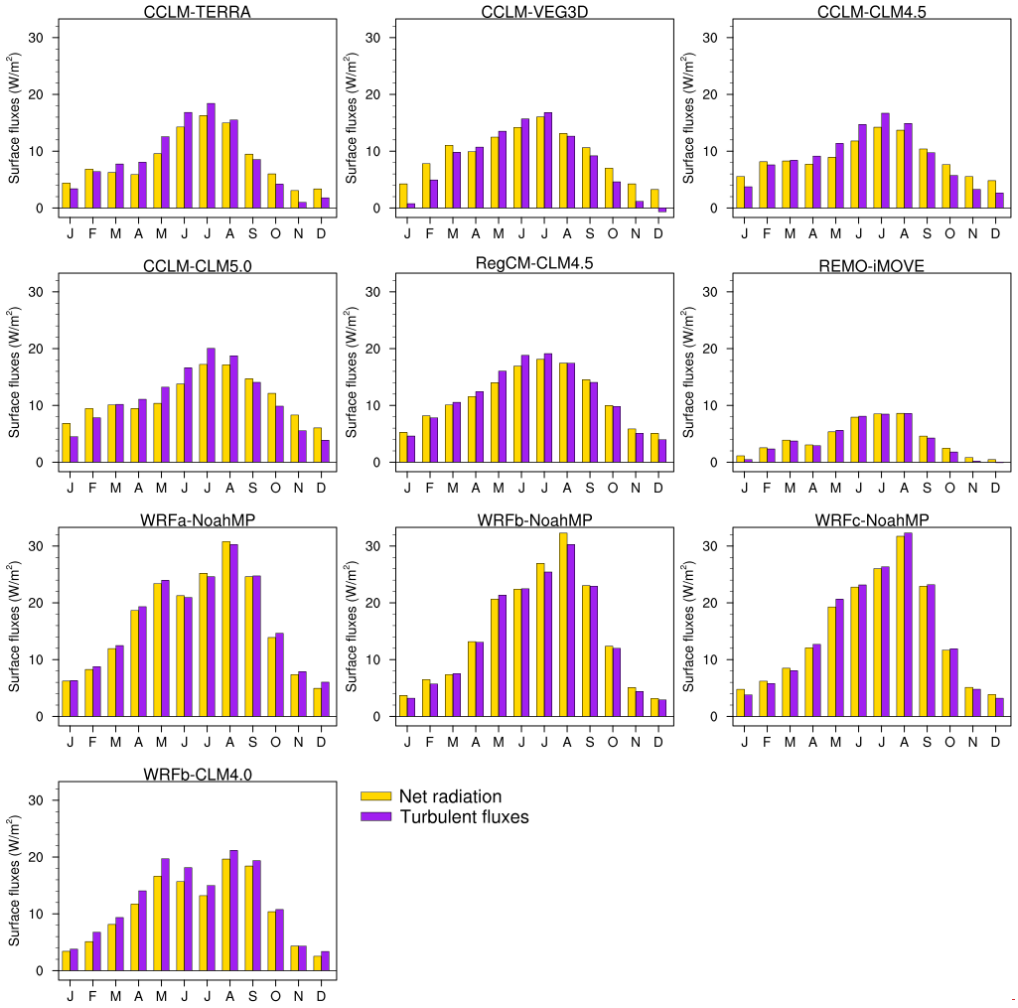

Figure 8: Mean monthly changes in net radiation and turbulent fluxes due to afforestation (FOREST minus GRASS) over Mediterranean. Turbulent fluxes are defined as the sum of sensible and latent heat fluxes.

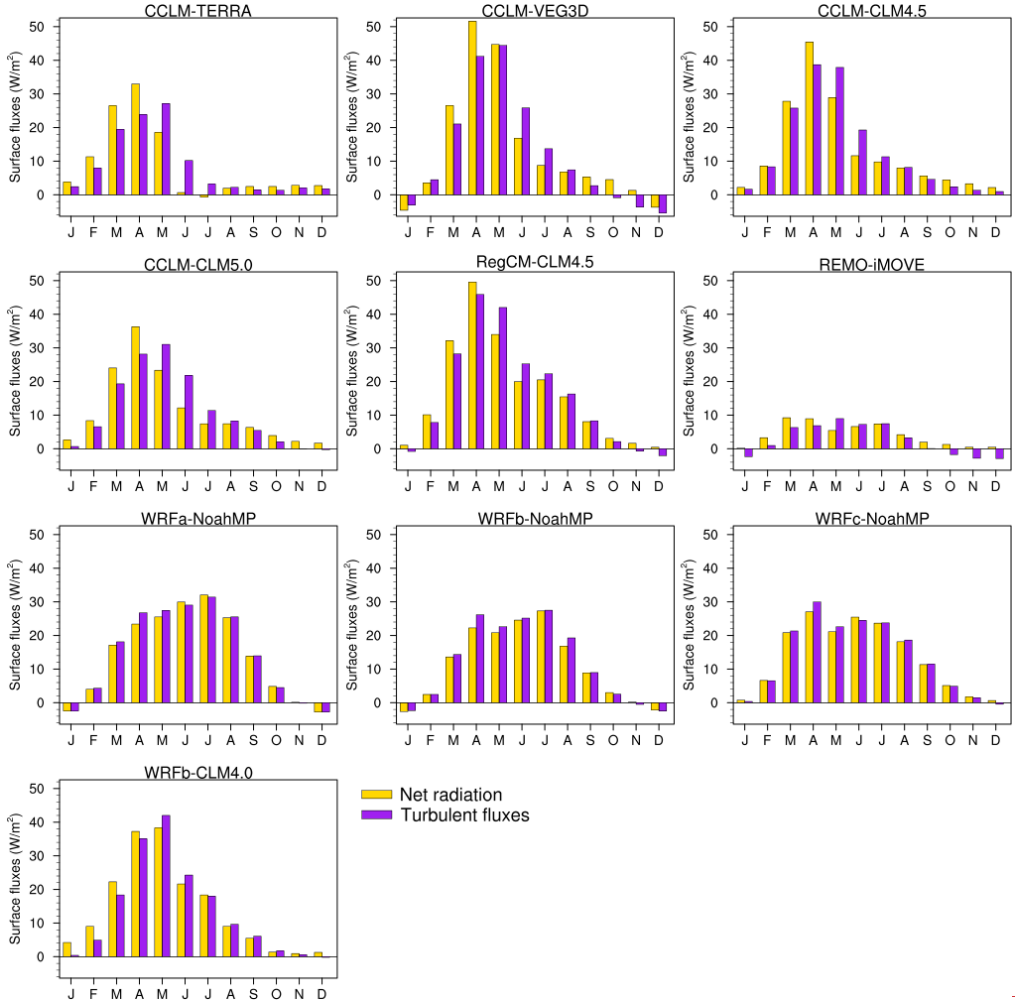

~~Figure 9: Mean monthly changes in net radiation and turbulent fluxes due to afforestation (FOREST minus GRASS) over Scandinavia. Turbulent fluxes are defined as the sum of sensible and latent heat fluxes.~~

3.3 Soil moisture

~~In addition to GHF, thermal diffusivity is also a parameter involved in the equation of the second heat conduction law and is linked with the temporal soil temperature variations. Soil moisture strongly regulates the thermal diffusivity within the soil column, since affecting the heat capacity of soil layers~~. The changes in soil moisture could also have key role in describing the simulated soil temperature response to afforestation, because they affect the thermal diffusivity within the soil column. It is expected that a drier (wetter) soil column would lead to a larger (smaller) AAST owing to its smaller(larger) heat capacity, when considering equal soil heat fluxes between the two experiments.

In **Figure ~~8~~10** we map the mean summer differences in soil moisture content (SMC) of~~in~~ the top 1 meter of the soil over the domain of interest (FOREST minus GRASS). A widespread soil moisture decrease is simulated over the biggest part of the domain, although with considerable variation in the magnitude of changes among the models. The choice of LSM produces a large spread of responses; within the sub-ensemble around CCLM the SMC change ranges from small decrease in CCLM-CLM4.5 and CCLM-CLM5.0 to more than -30 kg~~/~~m^{-2} for CCLM-TERRA in several regions ~~**(Figure S30)**~~. Differences in the magnitude of changes are also present between ~~the~~ WRFb-NoahMP and WRFb-CLM4.0. The atmospheric processes also affect the magnitude of afforestation effect on SMC; among the modelling systems sharing NoahMP, WRFa-NoahMP appears to be the most responsive, with changes exceeding -20 kg~~/~~m^{-2} in southern Europe. Further, many grid-cells over central and northern Europe exhibit SMC increase in WRFb-NoahMP and WRFc-NoahMP configurations, in contradiction to~~with~~ the extensive soil moisture reduction in WRFa-NoahMP.

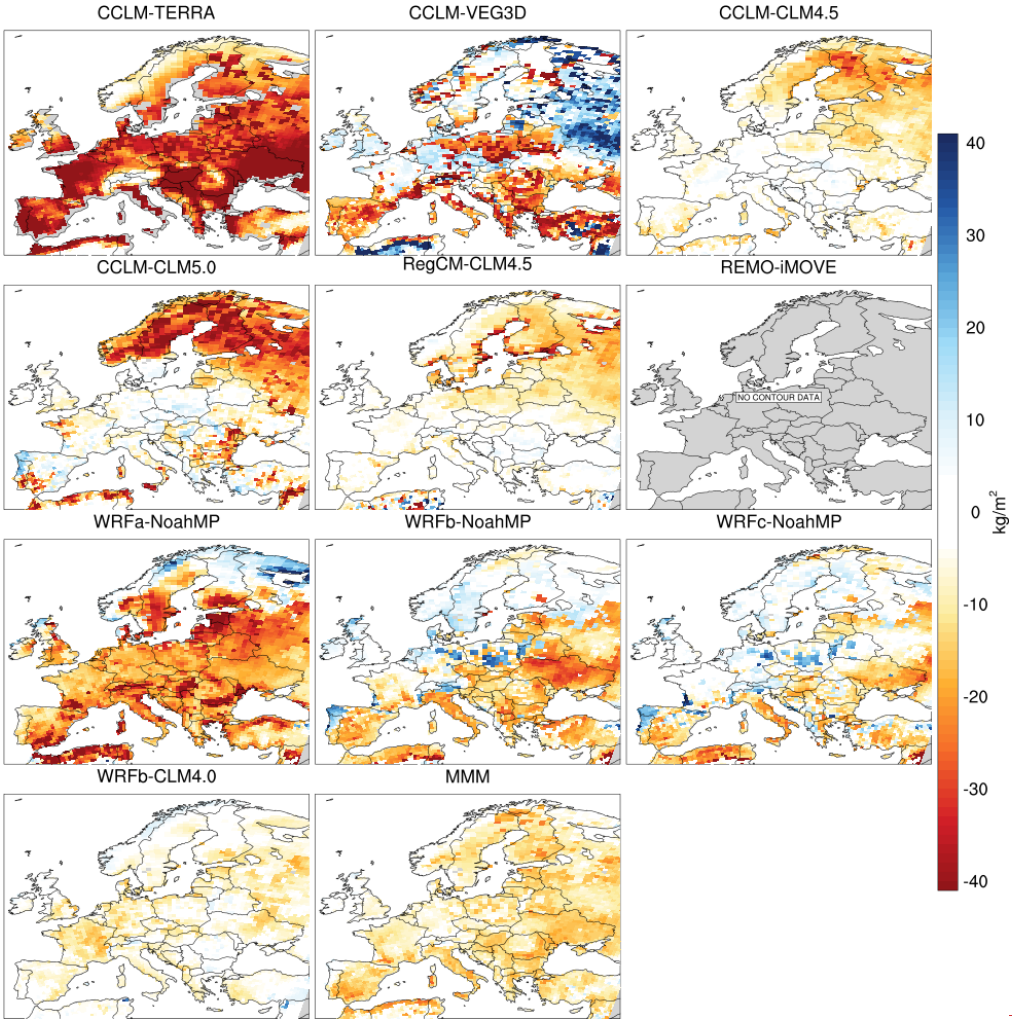

~~Figure 10: Afforestation (FOREST minus GRASS) impact on soil moisture content (kg m^{-2}) of the top 1 meter of the soil during summer. REMO-iMOVE is not included because it employed a bucket scheme for soil hydrology in the LUCAS Phase 1 experiments, which does not allow a separation of soil moisture into different layers.~~

The surface water balance (P-E), defined as the difference between precipitation (P) and total evapotranspiration (E), decreases with afforestation during summer in the majority of models over the whole Europe (**Figure S**18~~31~~). In most simulations, the

decrease in the terrestrial water budget originates from increased evapotranspiration rates with afforestation. In summer, high LAI values do not allow solar radiation to reach the ground surface, as a result soil evaporation is limited and transpiration dominates overall evapotranspiration (Bonan, 2008). Specific characteristics, such as the big leaf area, the deep roots, the great available energy due to low albedo and the mixing of the upper atmospheric boundary layer because of the high surface roughness, enhance the transpiration rate in forests. Although, CCLM-VEG3D and WRFa-NoahMP show positive sign of changes in water balance in regions of central and southern Europe, owing to decreased evapotranspiration with afforestation. This is probably linked with low atmospheric demands for hydrates in FOREST experiment of CCLM-VEG3D (Breil et al., 2021). In WRFa-NoahMP, the use of Grell-Freitas as convection scheme, exploits the transpiration-facilitating features of forests causing extreme soil drying from very early in summer. Therefore, the evapotranspiration rate lowers with afforestation, because the dry soil is not able to satisfy the atmospheric needs for hydrates.

The soil moisture changes with depth would indirectly reveal the afforestation effect on the evapotranspiration process during summer. The water uptake for transpiration occurs in different depths within the soil column for grasslands and forests. In grasslands, the soil water needed for transpiration is extracted from shallow layers, because the large fraction of their roots is located there, depleting the moisture of upper soil. On the other hand, forests have a deeper root distribution, thus consuming water from a bigger soil water reservoir. In **Figure 9~~11~~** we show the afforestation-induced soil moisture changes within the top 1 meter of the soil over Mediterranean and Scandinavia. Similar plots for the other sub-regions can be found in **Figure S19~~32~~** of the supplementary material. The heterogeneity of SMC changes with depth is evident in most models, especially in Mediterranean. In Scandinavia, distinct drying of the uppermost soil layers is shown by some models, especially CCLM-CLM4.5 and CCLM-CLM5.0, which is related to changes in water amounts from snow melt. The different structures of land models and the various descriptions of physiological characteristics of plants in LSMs, such as the root distributions, differentiate the pattern of SMC changes with depth among the simulations. Also, possible biases in the representation of surface fluxes potentially affect the afforestation effect on soil moisture. For example, in CCLM-TERRA the latent heat fluxes are strongly increased with afforestation, as discussed in previous studies (Davin et al., 2020; Breil et al., 2020), inducing intense drying of the soil column.

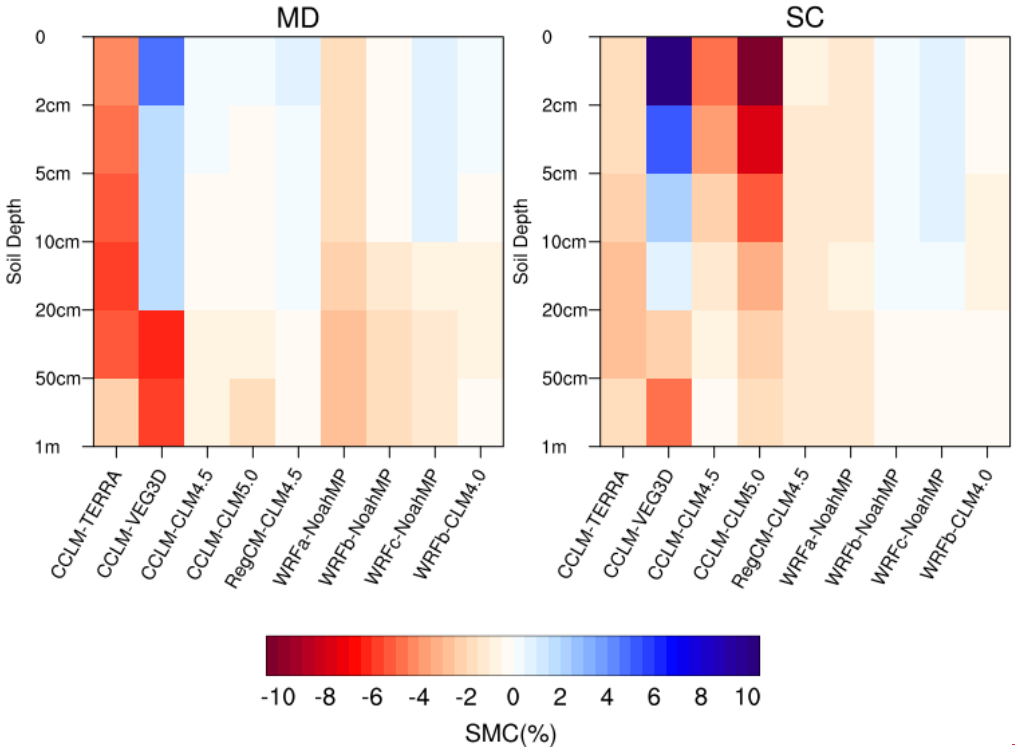

~~**Figure 11: Summer changes in soil moisture content (SMC) due to afforestation (FOREST minus GRASS) in the top 1 meter of the soil over Mediterranean (MD) and Scandinavia (SC).**~~

3.4 ~~Attributing~~ The origin of ~~the~~ inter-model spread in AAST ~~to AAGHF and SMC~~

~~With the aim to quantify the effect of AAGHF response and summer SMC changes on AAST response to afforestation, we conduct a linear regression analysis including the respective simulated responses over all the European sub-regions. Particularly, we use the changes in AAGHF and summer SMC as explanatory (independent) variables, to determine to what extent they influence the changes in AAST (dependent variable). When we regress both the explanatory variables against the AAST response, we find that the coefficient of multiple determination (R^2) is above 74% in most regions (**Figure 12**). The AAGHF response is the dominating factor which largely predicts the inter-model variance in AAST in most regions. On the other hand, the predictive ability of the summer SMC changes is not strong, with a small contribution to the explanation of the inter-spread in AAST over many regions of central Europe. In Scandinavia, the statistical approach shows low effectiveness in predicting the inter-model variance in AAST response. This is probably related to the fact that the ground in Scandinavia is~~

~~usually snow-covered in several months of year, thus the use of the residual of surface energy balance, as a proxy for the actual GHF output, is not suitable for describing the energy exchange on soil-atmosphere interface. Other variables, such as the changes in snow amount, could contribute to the explanation of AAST response in this region. Another caveat of the statistical approach constitutes the interaction between the changes in SMC and the impact of AAGHF changes on AAST response. The relatively drier soil conditions with afforestation reduce the heat capacity of soil column, and as a result attenuate the effect of AAGHF decrease on soil temperature. This interaction effect reduces the predictive ability of AAGHF response as explanatory variable.~~

~~Another question arises from our results is why the WRF-NoahMP modelling systems exhibit a positive sign of changes in AAST, while simulating a decrease in AAGHF with afforestation in line with the other simulations. The AAGHF sensitivity to afforestation is low in these simulations, because the radiative energy gain due to lower forest albedo is almost equal to the increased surface heat fluxes owing to higher forest surface roughness. The AAGHF decrease results from small GHF reduction during spring. Although, afforestation causes drier soil conditions during summer, which lead to smaller soil heat capacity. As a consequence, WRF-NoahMP members exhibit higher soil temperatures with afforestation in summer season and consequently larger annual soil temperature cycle, in contradiction to the majority of modelling systems where the AAGHF response mainly determines the AAST changes.~~

The widespread and homogeneous soil drying with afforestation, mentioned in previous section, is not consistent with the mixed AAST response. On the other hand, it is noted higher agreement between the pattern of changes in soil heating and in AAST. In section 3.2, we showed that the afforestation impact on radiative processes, such as the decrease in surface albedo, increase the available radiative energy at the surface. In parallel, the afforestation effect on non-radiative processes, removes a large part of thermal energy from surface to atmosphere in the form of sensible heat flux. The balance between these processes will determine if the surface energy input into the soil will be increased or decreased with afforestation in each RCM. However, the above biophysical processes are differently weighted across RCMs depending on land-use characteristics, like surface roughness, albedo,~~plant coverage~~, and LAI, which affect the turbulent mixing and the amount of the absorbed solar energy at the surface. Furthermore, the response of cloud fraction to afforestation is another important factor, which affects the soil heating, because of its impact on the incoming shortwave radiation at the surface.

With the aim to quantify the effect of changes in above mentioned quantities on the simulated AAST response to afforestation, we conduct a linear regression analysis over all the European sub-regions. More specifically, we use the mean summer changes in albedo, LAI, cloud fraction and soil moisture content as explanatory (independent) variables, to determine to what extent they influence the changes in AAST (dependent variable). When we regress all the explanatory variables against the simulated AAST response, we find that the coefficient of multiple determination (R^2) is above 80% in all regions, which indicates the key role of the selected drivers in shaping the effect of afforestation on soil temperature (**Figure 10**). In southern regions, Mediterranean and Iberian Peninsula, the albedo effect predicts the largest part of the inter-model spread in AAST response. Over regions of central Europe (Mid-Europe, eastern Europe, France, British Isles) the predictive ability of albedo changes remains strong, although the cloud fraction is the dominating factor which effectively explains the inter-model variance over

Formatted: Font: Bold

these regions. Soil moisture also contributes to the explanation of the inter-model spread in AAST over the regions of central Europe, although is not a dominating driver. In Scandinavia, the simulated AAST response is largely explained by differences in LAI across RCMs, with cloud fraction also substantially contributing to the prediction of the inter-model spread. The changes in LAI are potentially connected with the simulated cloud fraction response, since higher LAI values could facilitate the evaporation rates triggering an increase in cloud cover. This interaction effect between two or more physical processes which are used as explanatory variables constitutes a caveat of the used statistical approach, with result to reducing the effectiveness of the corresponding drivers in predicting the response of the dependent variable.

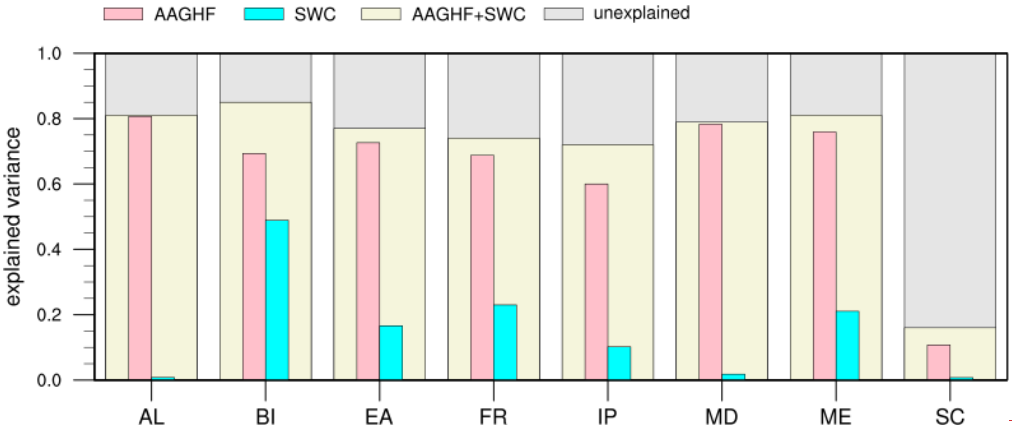

~~**Figure 12: The fraction of inter-model variance in AAST response (FOREST minus GRASS) explained by changes in AAGHF, soil moisture content (SMC) or both combined (AAGHF+SMC). Bars represent the coefficient of determination (R^2) values derived from linear regression analysis applied over each sub-region.**~~

3.5 FLUXNET paired sites

In this section, we compare the simulated impact on AAST with observational evidence of afforestation effect on soil temperature, based on ten FLUXNET paired sites. In winter, simulations and observations illustrate insignificant changes in soil temperature with afforestation (**Figure 1~~3~~**). T~~Although, t~~he magnitude of afforestation effect in the observations is amplified during summer, revealing a strong cooling up to -3 °C ~~K~~. The majority of models captures the seasonal pattern of changes in soil temperature and particularly the observed summer cooling, albeit with considerable variation in the magnitude of changes. CCLM-TERRA shows the largest changes in summer soil temperature (-5 °C ~~K~~), whereas WRFb-NoahMP and WRFc-NoahMP exhibit subtle summer cooling smaller than -1 °C ~~K~~. On the other hand, WRFa-NoahMP, CCLM-VEG3D and REMO-iMOVE do not capture the observed signal of changes in summer, simulating a warming. Especially REMO-iMOVE shows a yearly warming, opposite to the observed cooling throughout the year. According to the observations,

afforestation dampens the mean annual soil temperature range by almost -3 °C ~~K~~ which is qualitatively consistent with most RCMs, in which the decrease ranges from -5 °C ~~K~~ for CCLM-TERRA to -0.2 °C ~~K~~ for REMO-iMOVE. Notable exception is WRFa-NoahMP which exhibits a distinct increase greater than 1 °C ~~K~~, in contradiction to~~with~~ the observational evidence. Within the sub-ensemble of CCLM model, the selection of CLM (4.5 or 5.0) as the land component, refines the simulated impact of afforestation on AAST. Also, between the simulations sharing the same WRF atmospheric configuration (WRFb), the selection of CLM4.0 against NoahMP improves the representation of soil temperature response to afforestation.

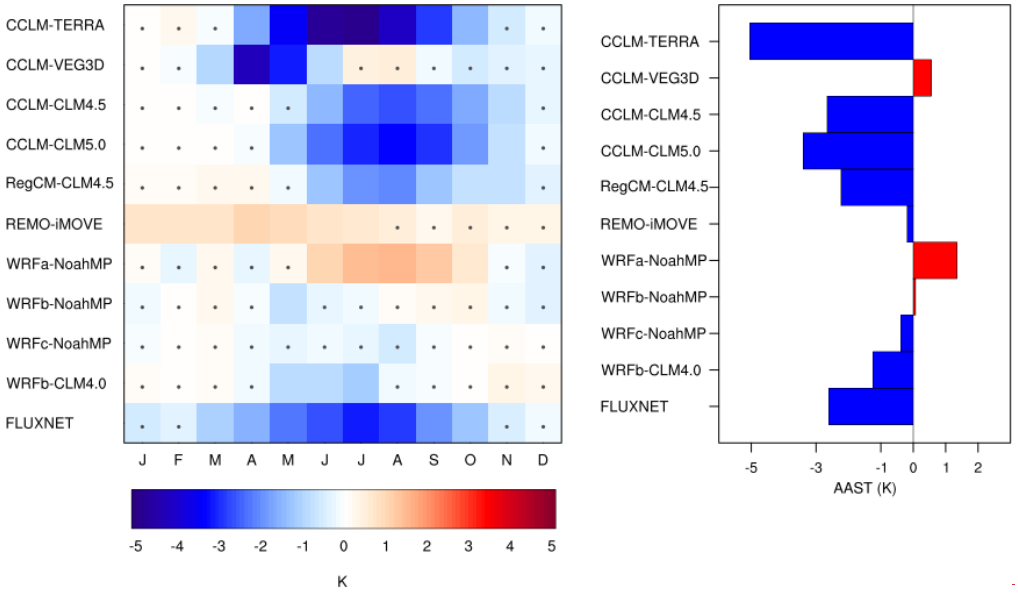

~~**Figure 13: Left: Observed and simulated impact of afforestation on mean monthly soil temperature. The dots indicate the differences which are insignificantly different from zero in a two-sided t-test at 95% confidence level. Right: The changes in AAST(K) due to afforestation across models and observations. The observational differences are averaged over all the paired FLUXNET sites (forest minus open land) and the simulated changes are averaged over the corresponding model grids (FOREST minus GRASS).**~~

4. Discussion & Conclusions

In this study, we employed the experimental design established within LUCAS FPS, to investigate the afforestation impact on soil temperature over the Euro-CORDEX domain. Two~~Particularly, t~~wo idealized land cover change experiments performed by an ensemble of ten RCMs, in which the European land surface is represented as fully covered by forest and grass, respectively. The majority of simulations showed a dampening of the annual soil temperature cycle with afforestation, owing

to changes in summer soil temperature. A large inter-model spread produced, ranging from -7 °C ~~K~~ to +2 °C ~~K~~ depending on model and region.

~~The dampening of the annual GHF cycle largely explained the inter-model variance in AAST response to afforestation in most regions. The AAGHF decrease was a robust feature among the models. An increase of the net shortwave radiation, owing to the lower forest albedo, induced higher GHF in winter. On the other hand, the enhanced surface heat fluxes in summer, owing to large surface roughness of forested areas, offset the radiative energy gain induced by the albedo effect, resulting in a decrease in summer GHF.~~

The changes in AAST with afforestation found to be consistent with summer changes in available energy to warm the ground across models and regions. In other words, RCMs which showed a ground cooling following afforestation, tend to simulate a reduction in surface energy input into the ground, and vice versa. What differentiates the sign of changes in soil heating across models, is the balance between two biophysical processes, which are greatly affected by afforestation. First, it is the increased available radiative energy at the surface, due to lower albedo in forests, and second it is the increased sum of turbulent heat fluxes (mostly sensible heat flux), owing to mixing-facilitating characteristics in forests, such as high LAI and surface roughness values, which enhance the heat exchange between ground and atmosphere. Although these physical processes are differently weighted in LSMs depending on land-use characteristics, such as surface albedo, surface roughness and LAI, while subsequent atmospheric feedbacks, such as the cloud cover changes, can influence the surface fluxes. Thus, the magnitude of afforestation effect on net shortwave radiation and on turbulent heat fluxes is differently pronounced across models. In six out of ten RCMs of the ensemble, the increased available radiative energy is compensated by the increased sum of turbulent heat fluxes, thus simulating a decrease in soil heating with afforestation and finally a reduction in soil temperature, while the opposite is true for the other four modelling systems. Finally, the changes in albedo, LAI, cloud fraction and soil moisture found to explain more than 80% of inter-model variance in AAST response in all sub-regions.

Previous studies which addressed the effects of LUC on soil temperature have reported similar results with the present work. ~~(~~Ni et al., 2019~~)~~ employed~~conducted an approach of~~ field monitoring on a landscape consisted of tree and grass covered ground, to investigate the soil temperature effects on root water uptake for a time period from July to November. They found that soil temperature under the grass-covered ground had larger fluctuations and slightly higher values compared to tree-covered ground in summer. ~~(~~Lozano-Parra et al., 2018~~)~~ studied the combined effect of soil moisture and vegetation cover on soil temperature over three dryland areas of the Iberian Peninsula for two hydrological years. Under dry conditions, they found smaller daily amplitudes of soil temperature below the tree canopies than in grasslands. ~~(~~Longobardi et al., 2016~~)~~ used a global climate model to investigate the climate sensitivity to various rates of deforestation across the globe. According to their results, deforestation warmed the soils of the mid latitudes, because of a reduction in sensible heat fluxes that offset the induced albedo increase. Lastly, ~~(~~MacDougall and Beltrami, 2017~~)~~ conducted a GCM experiment to study the historical deforestation impact on subsurface temperatures on global scale. They found that a soil temperature increase remains present for centuries following the deforestation, originated from the reduction of surface energy fluxes towards the atmosphere.

In line with recent findings from observations and model-based studies (Jia et al., 2017; Ren et al., 2018; Zhang et al., 2018; Li et al., 2018), we found that afforestation induced a widespread soil moisture reduction in summer, implying smaller soil heat capacity. This was also a robust feature among the models, albeit with a considerable range in the magnitude of changes. Soil moisture decrease with afforestation resulted from large drying of deep layers, related to the fact that forests and grasslands extract soil water for transpiration process from different soil depths. ~~Furthermore, soil moisture decline determined the increase of summer soil temperature and consequently the increased AAST, in three out of the ten ensemble members, in which the summer GHF sensitivity to afforestation was low. In general, soil moisture changes were not the dominant factor in determining the direction of changes in AAST, moderating only the impact of AAGHF on AAST.~~Although, the homogeneous soil drying and thus the smaller soil heat capacity is not consistent with the afforestation-induced decrease of soil temperature in the majority of models, explaining only a small part of inter-model variance in AAST response in regions of central Europe.

Based on paired observations from FLUXNET dataset, we evaluated the simulated soil temperature response to afforestation. The vast majority of models agreed with the observational evidence that showed a summer ground cooling in forested areas compared to open land. The paired sites exhibited a mean reduction of -3 ^{o}C ~~K~~ in AAST, while the simulated response varied from -5 ^{o}C ~~K~~ to 1 ^{o}C~~K~~.

The current ensemble enables us to address the role of atmospheric and land processes in the representation of biophysical forcing of land cover change, since it involves simulations which share the same atmospheric model coupled to different land components, or share the same LSM with different atmospheric set-ups. The switch from CCLM to RegCM when both coupled to CLM4.5 did not induce important changes in model results, implying the dominance of land processes in these simulations. ~~Though, A~~among the suite of models which share the NoahMP LSM, the atmospheric configuration selected for WRFb-NoahMP and WRFc-NoahMP significantly refined the afforestation effect on soil temperature, compared to WRFa-NoahMP. Future studies should focus on the evaluation of model performances, similar to ~~(~~Katragkou et al., 2015~~)~~ and ~~(~~Constantinidou et al., 2020a~~)~~, in order to identify the origins of systematic biases and improve the representation of climate processes in simulations. Moreover, our results stress the crucial role of LSM in the simulation of the biophysical effects of afforestation on soil conditions. Among the LSMs~~land models~~ coupled to the CCLM model, the choice of CLM significantly improves the representation of afforestation impact on AAST. Also, WRF coupled to CLM4.0 agreed better with observations than WRF coupled to NoahMP. Another issue is the~~Last,~~ problematic behaviours in model performances stemming ~~probably derive~~ from unrealistic descriptions of the physical plant functioning in LSMs. ~~(~~Meier et al., 2018~~)~~ improved the representation of the evapotranspiration with land cover change in CLM4.5, modifying parameters related to transpiration process, such as the root distribution and water uptake formulation.

Research has accounted for the contribution of historical deforestation to present climate conditions. Last years~~Nowadays~~, governments and non-governmental organizations are planning re/afforestation programs around the world with the purpose to mitigate the negative effects of anthropogenic activities on climate. With our study, we aspire to contribute to the deeper understanding of the scientific community on the biophysical effects of afforestation on soil conditions. Future studies focused on the consequences of afforestation from biological or chemical aspect, are encouraged to consider our results, in order to

draw comprehensive conclusions on important climate processes in which afforestation is involved, such as the carbon sequestration and microbial respiration.

Code and data availability

We used soil temperature data from the FLUXNET2015 Tier Two dataset, which can be accessed at the website (https://fluxnet.org/)(last access: 05 March 2021, (Pastorello et al., 2020)). Simulations were forced by the ERA-Interim reanalysis data set (https://www.ecmwf.int/en/forecasts/datasets/reanalysis-datasets/era-interim) (last access:08 March 2021, (Dee et al., 2011). ~~Vegetation maps applied in FOREST and GRASS experiments can be found in (Davin et al., 2020)~~. The source code of the Weather Research and Forecasting Model (WRF) is available by UCAR/NCAR and can be accessed at https://www.mmm.ucar.edu/weather-research-and-forecasting-model (last access: 08 March 2021, (Skamarock et al., 2008)). The documentation of COSMO-Model is available at the following link (https://www.dwd.de/EN/ourservices/cosmo_documentation/cosmo_documentation.html), although a license is required for access (http://www.cosmo-model.org/content/consortium/licencing.htm). RegCM4 model is distributed from https://github.com/ictp-esp/RegCM (last access: 08 March 2021, (Giorgi et al., 2012)). The source code of REMO model is available on request from the Climate Service Center Germany (contact@remo-rcm.de) (Wilhelm et al., 2014). ~~Detailed description on the parameterization schemes and atmospheric settings used from each modelling system can be found in (Davin et al., 2020)~~. All the scripts and data upon which this study is based can be accessed at the link: 10.5281/zenodo.4588724 .

Field Code Changed

Author contributions

GS, EK and ELD designed the research. GS, EK, ELD, RM, DR, MB, RMC, PH, LJ, PM, PMMS, SS, MHT and KWS performed the RCM simulations. GS analyzed the data and wrote the paper with inputs from all coauthors.

Competing interests.

The authors declare that they have no conflict of interest.

Acknowledgements

The author gratefully acknowledges the Swiss Confederation for financial support through Government Excellence Scholarship for the academic year 2019-2020. The author thanks Prof. Sonia I. Seneviratne for the fruitful discussions on the progress of this study. The work of GS and EK was supported by computational time granted from the National Infrastructures for Research and Technology S.A. (GRNET S.A.) in the National HPC facility - ARIS - under project ID pr005025 and pr007033_thin. ELD and RM acknowledge support from the Swiss National Science Foundation (SNSF) through the

CLIMPULSE project and thanks the Swiss National Supercomputing Centre (CSCS) for providing computing resources. Rita M. Cardoso and Pedro M. M. Soares acknowledge the projects LEADING (PTDC/CTA-MET/28914/2017) and FCT-UID/GEO/50019/2019 – Instituto Dom Luiz. Peter Hoffmann is funded by the Climate Service Center Germany (GERICS) of the Helmholtz-Zentrum ~~Geesthacht~~ Hereon in the frame of the HICSS (Helmholtz-Institut Climate Service Science) project LANDMATE. Lisa L. Jach, and Kirsten Warrach-Sagi acknowledge support by the state of Baden-Württemberg through bwHPC and thank the Anton and Petra Ehrmann-Stiftung Research Training Group "Water-People-Agriculture" for financial support. Susanna Strada has been supported by the TALENTS3 Fellowship Programme (FP code 1718349004) funded by the autonomous region Friuli Venezia Giulia via the European Social Fund (Operative Regional Programme 2014–2020) and administered by the AREA Science Park (Padriciano, Italy). Merja H. Tölle thanks the German Climate Computing Center (DKRZ) for providing computing resources, the CLM-community for support and acknowledges the ~~CCLM-TERRA simulations were performed at the German Climate Computing Center (DKRZ) through support from the Federal Ministry of Education and Research in Germany (BMBF). Merja H. Tölle acknowledges the~~ funding of the German Research Foundation (DFG) through grant 401857120. The authors gratefully acknowledge the WCRP CORDEX Flagship Pilot Study LUCAS "Land use and Climate Across Scales~~"~~", and the research data exchange infrastructure and services provided by the Jülich Supercomputing Centre, Germany, as part of the Helmholtz Data Federation initiative.

Financial support

The research work was supported by the Hellenic Foundation for Research and Innovation (HFRI) under the HFRI PhD Fellowship grant (Fellowship Number: 1359).

References

Belušić, D., Fuentes-Franco, R., Strandberg, G., and Jukimenko, A.: Afforestation reduces cyclone intensity and precipitation extremes over Europe, Environ. Res. Lett., 14, 074009, https://doi.org/10.1088/1748-9326/ab23b2, 2019.

Betts, R. A.: Offset of the potential carbon sink from boreal forestation by decreases in surface albedo, Nature, 408, 187–190, https://doi.org/10.1038/35041545, 2000.

Boisier, J. P., Noblet-Ducoudré, N. de, Pitman, A. J., Cruz, F. T., Delire, C., Hurk, B. J. J. M. van den, Molen, M. K. van der, Müller, C., and Voldoire, A.: Attributing the impacts of land-cover changes in temperate regions on surface temperature and heat fluxes to specific causes: Results from the first LUCID set of simulations, 117, https://doi.org/10.1029/2011JD017106, 2012.

Bonan, G. B.: Forests and Climate Change: Forcings, Feedbacks, and the Climate Benefits of Forests, Science, 320, 1444–1449, https://doi.org/10.1126/science.1155121, 2008.

Breil, M., Schädler, G., and Laube, N.: An Improved Soil Moisture Parametrization for Regional Climate Simulations in Europe, https://doi.org/10.1029/2018JD028704, 2018.

Breil, M., Rechid, D., Davin, E. L., Noblet-Ducoudré, N. de, Katragkou, E., Cardoso, R. M., Hoffmann, P., Jach, L. L., Soares, P. M. M., Sofiadis, G., Strada, S., Strandberg, G., Tölle, M. H., and Warrach-Sagi, K.: The Opposing Effects of Reforestation and Afforestation on the Diurnal Temperature Cycle at the Surface and in the Lowest Atmospheric Model Level in the European Summer, 33, 9159–9179, https://doi.org/10.1175/JCLI-D-19-0624.1, 2020.

Breil, M., Davin, E. L., and Rechid, D.: What determines the sign of the evapotranspiration response to afforestation in European summer?, 18, 1499–1510, https://doi.org/10.5194/bg-18-1499-2021, 2021.

Broucke, S. V., Luyssaert, S., Davin, E. L., Janssens, I., and Lipzig, N. van: New insights in the capability of climate models to simulate the impact of LUC based on temperature decomposition of paired site observations, 120, 5417–5436, https://doi.org/10.1002/2015JD023095, 2015.

Cardoso, R. M., Soares, P. M. M., Miranda, P. M. A., and Belo-Pereira, M.: WRF high resolution simulation of Iberian mean and extreme precipitation climate, 33, 2591–2608, https://doi.org/10.1002/joc.3616, 2013.

Chen, L., Dirmeyer, P. A., Guo, Z., and Schultz, N. M.: Pairing FLUXNET sites to validate model representations of land-use/land-cover change, 22, 111–125, https://doi.org/10.5194/hess-22-111-2018, 2018.

Cherubini, F., Huang, B., Hu, X., Tölle, M. H., and Strømman, A. H.: Quantifying the climate response to extreme land cover changes in Europe with a regional model, Environ. Res. Lett., 13, 074002, https://doi.org/10.1088/1748-9326/aac794, 2018.

Christensen, J. H. and Christensen, O. B.: A summary of the PRUDENCE model projections of changes in European climate by the end of this century, Climatic Change, 81, 7–30, https://doi.org/10.1007/s10584-006-9210-7, 2007.

Claussen, M., Brovkin, V., and Ganopolski, A.: Biogeophysical versus biogeochemical feedbacks of large-scale land cover change, 28, 1011–1014, https://doi.org/10.1029/2000GL012471, 2001.

Constantinidou, K., Hadjinicolaou, P., Zittis, G., and Lelieveld, J.: Performance of Land Surface Schemes in the WRF Model for Climate Simulations over the MENA-CORDEX Domain, Earth Syst Environ, 4, 647–665, https://doi.org/10.1007/s41748-020-00187-1, 2020a.

Constantinidou, K., Hadjinicolaou, P., Zittis, G., and Lelieveld, J.: Sensitivity of simulated climate over the MENA region related to different land surface schemes in the WRF model, Theor Appl Climatol, 141, 1431–1449, https://doi.org/10.1007/s00704-020-03258-5, 2020b.

Davin, E. L. and de Noblet-Ducoudre, N.: Climatic impact of global-scale Deforestation: Radiative versus nonradiative processes, https://doi.org/10.1175/2009JCLI3102.1, 2010.

Davin, E. L., Noblet-Ducoudré, N. de, and Friedlingstein, P.: Impact of land cover change on surface climate: Relevance of the radiative forcing concept, 34, https://doi.org/10.1029/2007GL029678, 2007.

Davin, E. L., Rechid, Di., Breil, M., Cardoso, R. M., Coppola, E., Hoffmann, P., Jach, L. L., Katragkou, E., De Noblet-Ducoudré, N., Radtke, K., Raffa, M., Soares, P. M. M., Sofiadis, G., Strada, S., Strandberg, G., Tölle, M. H., Warrach-Sagi, K., and Wulfmeyer, V.: Biogeophysical impacts of forestation in Europe: First results from the LUCAS (Land Use and Climate across Scales) regional climate model intercomparison, https://doi.org/10.5194/esd-11-183-2020, 2020.

Dee, D. P., Uppala, S. M., Simmons, A. J., Berrisford, P., Poli, P., Kobayashi, S., Andrae, U., Balmaseda, M. A., Balsamo, G., Bauer, P., Bechtold, P., Beljaars, A. C. M., Berg, L. van de, Bidlot, J., Bormann, N., Delsol, C., Dragani, R., Fuentes, M., Geer, A. J., Haimberger, L., Healy, S. B., Hersbach, H., Hólm, E. V., Isaksen, L., Kållberg, P., Köhler, M., Matricardi, M., McNally, A. P., Monge-Sanz, B. M., Morcrette, J.-J., Park, B.-K., Peubey, C., Rosnay, P. de, Tavolato, C., Thépaut, J.-N., and Vitart, F.: The ERA-Interim reanalysis: configuration and performance of the data assimilation system, 137, 553–597, https://doi.org/10.1002/qj.828, 2011.

Devaraju, N., Bala, G., and Nemani, R.: Modelling the influence of land-use changes on biophysical and biochemical interactions at regional and global scales, 38, 1931–1946, https://doi.org/10.1111/pce.12488, 2015.

Doms, G., Förstner, J., Heise, E., Herzog, H.-J., Mironov, D., Raschendorfer, M., Reinhardt, T., Ritter, Schrodin, B. R., Schulz, J.-P., and Vogel, G.: A Description of the Nonhydrostatic Regional Model LM, Part II: Physical Parameterization. DWD, 2013.

Duveiller, G., Hooker, J., and Cescatti, A.: The mark of vegetation change on Earth's surface energy balance, 9, 679, https://doi.org/10.1038/s41467-017-02810-8, 2018.

Farouki, O. T.: The thermal properties of soils in cold regions, Cold Regions Science and Technology, 5, 67–75, https://doi.org/10.1016/0165-232X(81)90041-0, 1981.

Gálos, B., Hagemann, S., Hänsler, A., Kindermann, G., Rechid, D., Sieck, K., Teichmann, C., and Jacob, D.: Case study for the assessment of the biogeophysical effects of a potential afforestation in Europe, Carbon Balance Manage, 8, 3, https://doi.org/10.1186/1750-0680-8-3, 2013.

Giorgi, F.: Thirty Years of Regional Climate Modeling: Where Are We and Where Are We Going next?, 124, 5696–5723, https://doi.org/10.1029/2018JD030094, 2019.

Giorgi, F., Coppola, E., Solmon, F., Mariotti, L., Sylla, M., Bi, X., Elguindi, N., Diro, G., Nair, V., Giuliani, G., Turuncoglu, U., Cozzini, S., Güttler, I., O'Brien, T., Tawfik, A., Shalaby, A., Zakey, A., Steiner, A., Stordal, F., Sloan, L., and Brankovic, C.: RegCM4: model description and preliminary tests over multiple CORDEX domains, Clim. Res., 52, 7–29, https://doi.org/10.3354/cr01018, 2012.

Grassi, G., House, J., Dentener, F., Federici, S., den Elzen, M., and Penman, J.: The key role of forests in meeting climate targets requires science for credible mitigation, 7, 220–226, https://doi.org/10.1038/nclimate3227, 2017.

Hong, S.-Y., Noh, Y., and Dudhia, J.: A New Vertical Diffusion Package with an Explicit Treatment of Entrainment Processes, 134, 2318–2341, https://doi.org/10.1175/MWR3199.1, 2006.

Jacob, D., Petersen, J., Eggert, B., Alias, A., Christensen, O. B., Bouwer, L. M., Braun, A., Colette, A., Déqué, M., Georgievski, G., Georgopoulou, E., Gobiet, A., Menut, L., Nikulin, G., Haensler, A., Hempelmann, N., Jones, C., Keuler, K., Kovats, S., Kröner, N., Kotlarski, S., Kriegsmann, A., Martin, E., van Meijgaard, E., Moseley, C., Pfeifer, S., Preuschmann, S., Radermacher, C., Radtke, K., Rechid, D., Rounsevell, M., Samuelsson, P., Somot, S., Soussana, J.-F., Teichmann, C., Valentini, R., Vautard, R., Weber, B., and Yiou, P.: EURO-CORDEX: new high-resolution climate change projections for European impact research, Reg Environ Change, 14, 563–578, https://doi.org/10.1007/s10113-013-0499-2, 2014.

Jacob, D., Teichmann, C., Sobolowski, S., Katragkou, E., Anders, I., Belda, M., Benestad, R., Boberg, F., Buonomo, E., Cardoso, R. M., Casanueva, A., Christensen, O. B., Christensen, J. H., Coppola, E., De Cruz, L., Davin, E. L., Dobler, A., Domínguez, M., Fealy, R., Fernandez, J., Gaertner, M. A., García-Díez, M., Giorgi, F., Gobiet, A., Goergen, K., Gómez-Navarro, J. J., Alemán, J. J. G., Gutiérrez, C., Gutiérrez, J. M., Güttler, I., Haensler, A., Halenka, T., Jerez, S., Jiménez-Guerrero, P., Jones, R. G., Keuler, K., Kjellström, E., Knist, S., Kotlarski, S., Maraun, D., van Meijgaard, E., Mercogliano, P.,

Montávez, J. P., Navarra, A., Nikulin, G., de Noblet-Ducoudré, N., Panitz, H.-J., Pfeifer, S., Piazza, M., Pichelli, E., Pietikäinen, J.-P., Prein, A. F., Preuschmann, S., Rechid, D., Rockel, B., Romera, R., Sánchez, E., Sieck, K., Soares, P. M. M., Somot, S., Srnec, L., Sørland, S. L., Termonia, P., Truhetz, H., Vautard, R., Warrach-Sagi, K., and Wulfmeyer, V.: Regional climate downscaling over Europe: perspectives from the EURO-CORDEX community, Reg Environ Change, 20, 51, https://doi.org/10.1007/s10113-020-01606-9, 2020.

Jia, X., Shao, M., Zhu, Y., and Luo, Y.: Soil moisture decline due to afforestation across the Loess Plateau, China, Journal of Hydrology, 546, 113–122, https://doi.org/10.1016/j.jhydrol.2017.01.011, 2017.

Johansen, O.: Thermal conductivity of soils, Tech. Rep., DTIC Document, 1977.

Katragkou, E., García-Díez, M., Vautard, R., Sobolowski, S., Zanis, P., Alexandri, G., Cardoso, R. M., Colette, A., Fernandez, J., Gobiet, A., Goergen, K., Karacostas, T., Knist, S., Mayer, S., Soares, P. M. M., Pytharoulis, I., Tegoulias, I., Tsikerdekis, A., and Jacob, D.: Regional climate hindcast simulations within EURO-CORDEX: evaluation of a WRF multi-physics ensemble, 8, 603–618, https://doi.org/10.5194/gmd-8-603-2015, 2015.

Laguë, M. M. and Swann, A. L. S.: Progressive Midlatitude Afforestation: Impacts on Clouds, Global Energy Transport, and Precipitation, 29, 5561–5573, https://doi.org/10.1175/JCLI-D-15-0748.1, 2016.

Lawrence, D. M., Fisher, R. A., Koven, C. D., Oleson, K. W., Swenson, S. C., Bonan, G., Collier, N., Ghimire, B., Kampenhout, L. van, Kennedy, D., Kluzek, E., Lawrence, P. J., Li, F., Li, H., Lombardozzi, D., Riley, W. J., Sacks, W. J., Shi, M., Vertenstein, M., Wieder, W. R., Xu, C., Ali, A. A., Badger, A. M., Bisht, G., Broeke, M. van den, Brunke, M. A., Burns, S. P., Buzan, J., Clark, M., Craig, A., Dahlin, K., Drewniak, B., Fisher, J. B., Flanner, M., Fox, A. M., Gentine, P., Hoffman, F., Keppel-Aleks, G., Knox, R., Kumar, S., Lenaerts, J., Leung, L. R., Lipscomb, W. H., Lu, Y., Pandey, A., Pelletier, J. D., Perket, J., Randerson, J. T., Ricciuto, D. M., Sanderson, B. M., Slater, A., Subin, Z. M., Tang, J., Thomas, R. Q., Martin, M. V., and Zeng, X.: The Community Land Model Version 5: Description of New Features, Benchmarking, and Impact of Forcing Uncertainty, 11, 4245–4287, https://doi.org/10.1029/2018MS001583, 2019.

Lejeune, Q., Davin, E. L., Guillod, B. P., and Seneviratne, S. I.: Influence of Amazonian deforestation on the future evolution of regional surface fluxes, circulation, surface temperature and precipitation, Clim Dyn, 44, 2769–2786, https://doi.org/10.1007/s00382-014-2203-8, 2015.

Lejeune, Q., Davin, E. L., Gudmundsson, L., Winckler, J., and Seneviratne, S. I.: Historical deforestation locally increased the intensity of hot days in northern mid-latitudes, https://doi.org/10.1038/s41558-018-0131-z, 2018.

Li, Y., Zhao, M., Mildrexler, D. J., Motesharrei, S., Mu, Q., Kalnay, E., Zhao, F., Li, S., and Wang, K.: Potential and Actual impacts of deforestation and afforestation on land surface temperature, 121, 14,372-14,386, https://doi.org/10.1002/2016JD024969, 2016.

Li, Y., Piao, S., Li, L. Z. X., Chen, A., Wang, X., Ciais, P., Huang, L., Lian, X., Peng, S., Zeng, Z., Wang, K., and Zhou, L.: Divergent hydrological response to large-scale afforestation and vegetation greening in China, 4, eaar4182, https://doi.org/10.1126/sciadv.aar4182, 2018.

Longobardi, P., Montenegro, A., Beltrami, H., and Eby, M.: Deforestation Induced Climate Change: Effects of Spatial Scale, PLOS ONE, 11, e0153357, https://doi.org/10.1371/journal.pone.0153357, 2016.

Lozano-Parra, J., Pulido, M., Lozano-Fondón, C., and Schnabel, S.: How do Soil Moisture and Vegetation Covers Influence Soil Temperature in Drylands of Mediterranean Regions?, 10, 1747, https://doi.org/10.3390/w10121747, 2018.

MacDougall, A. H. and Beltrami, H.: Impact of deforestation on subsurface temperature profiles: implications for the borehole paleoclimate record, Environ. Res. Lett., 12, 074014, https://doi.org/10.1088/1748-9326/aa7394, 2017.

Meier, R., Davin, E. L., Lejeune, Q., Hauser, M., Li, Y., Martens, B., Schultz, N. M., Sterling, S., and Thiery, W.: Evaluating and improving the Community Land Model's sensitivity to land cover, 15, 4731–4757, https://doi.org/10.5194/bg-15-4731-2018, 2018.

Meier, R., Davin, E. L., Swenson, S. C., Lawrence, D. M., and Schwaab, J.: Biomass heat storage dampens diurnal temperature variations in forests, Environ. Res. Lett., 14, 084026, https://doi.org/10.1088/1748-9326/ab2b4e, 2019.

Mooney, P. A., Rechid, D., Davin, E. L., Katragkou, E., de Noblet-Ducoudré, N., Breil, M., Cardoso, R. M., Daloz, A. S., Hoffmann, P., Lima, D. C. A., Meier, R., Soares, P. M. M., Sofiadis, G., Strada, S., Strandberg, G., Toelle, M. H., and Lund, M. T.: Land-atmosphere interactions in sub-polar and alpine climates in the CORDEX FPS LUCAS models: Part II. The role of changing vegetation, 1–22, https://doi.org/10.5194/tc-2021-291, 2021.

Nakanishi, M. and Niino, H.: Development of an Improved Turbulence Closure Model for the Atmospheric Boundary Layer, Journal of the Meteorological Society of Japan, 87, 895–912, https://doi.org/10.2151/jmsj.87.895, 2009.

Ni, J., Cheng, Y., Wang, Q., Ng, C. W. W., and Garg, A.: Effects of vegetation on soil temperature and water content: Field monitoring and numerical modelling, Journal of Hydrology, 571, 494–502, https://doi.org/10.1016/j.jhydrol.2019.02.009, 2019.

Noblet-Ducoudré, N. de, Boisier, J.-P., Pitman, A., Bonan, G. B., Brovkin, V., Cruz, F., Delire, C., Gayler, V., Hurk, B. J. J. M. van den, Lawrence, P. J., Molen, M. K. van der, Müller, C., Reick, C. H., Strengers, B. J., and Voldoire, A.: Determining Robust Impacts of Land-Use-Induced Land Cover Changes on Surface Climate over North America and Eurasia: Results from the First Set of LUCID Experiments, 25, 3261–3281, https://doi.org/10.1175/JCLI-D-11-00338.1, 2012.

Oleson, K., Lawrence, D., Bonan, G., Drewniak, B., Huang, M., Koven, C., Levis, S., Li, F., Riley, W., Subin, Z., Swenson, S., Thornton, P., Bozbiyik, A., Fisher, R., Heald, C., Kluzek, E., Lamarque, J.-F., Lawrence, P., Leung, L., Lipscomb, W., Muszala, S., Ricciuto, D., Sacks, W., Sun, Y., Tang, J., and Yang, Z.-L.: Technical description of version 4.5 of the Community Land Model (CLM), UCAR/NCAR, https://doi.org/10.5065/D6RR1W7M, 2013.

Oleson, K. W., Lawrence, D. M., Bonan, G. B., Flanner, M. G., Kluzek, E., Lawrence, P. J., Levis, S., Swenson, S. C., Thornton, P. E., Dai, A., Decker, M., Dickinson, R., Feddema, J., Heald, C. L., Hoffman, F., Lamarque, J.-F., Mahowald, N., Niu, G.-Y., Qian, T., Randerson, J., Running, S., Sakaguchi, K., Slater, A., Stöckli, R., Wang, A., Yang, Z.-L., Zeng, X., and Zeng, X.: Technical Description of version 4.0 of the Community Land Model (CLM), 2010.

Pastorello, G., Trotta, C., Canfora, E., Chu, H., Christianson, D., Cheah, Y.-W., Poindexter, C., Chen, J., Elbashandy, A., Humphrey, M., Isaac, P., Polidori, D., Reichstein, M., Ribeca, A., van Ingen, C., Vuichard, N., Zhang, L., Amiro, B., Ammann, C., Arain, M. A., Ardö, J., Arkebauer, T., Arndt, S. K., Arriga, N., Aubinet, M., Aurela, M., Baldocchi, D., Barr, A., Beamesderfer, E., Marchesini, L. B., Bergeron, O., Beringer, J., Bernhofer, C., Berveiller, D., Billesbach, D., Black, T. A., Blanken, P. D., Bohrer, G., Boike, J., Bolstad, P. V., Bonal, D., Bonnefond, J.-M., Bowling, D. R., Bracho, R., Brodeur, J., Brümmer, C., Buchmann, N., Burban, B., Burns, S. P., Buysse, P., Cale, P., Cavagna, M., Cellier, P., Chen, S., Chini, I., Christensen, T. R., Cleverly, J., Collalti, A., Consalvo, C., Cook, B. D., Cook, D., Coursolle, C., Cremonese, E., Curtis, P. S., D'Andrea, E., da Rocha, H., Dai, X., Davis, K. J., Cinti, B. D., Grandcourt, A. de, Ligne, A. D., De Oliveira, R. C., Delpierre, N., Desai, A. R., Di Bella, C. M., Tommasi, P. di, Dolman, H., Domingo, F., Dong, G., Dore, S., Duce, P., Dufrêne, E., Dunn, A., Dušek, J., Eamus, D., Eichelmann, U., ElKhidir, H. A. M., Eugster, W., Ewenz, C. M., Ewers, B., Famulari, D., Fares, S., Feigenwinter, I., Feitz, A., Fensholt, R., Filippa, G., Fischer, M., Frank, J., Galvagno, M., et al.: The FLUXNET2015 dataset and the ONEFlux processing pipeline for eddy covariance data, 7, 225, https://doi.org/10.1038/s41597-020-0534-3, 2020.

Perugini, L., Caporaso, L., Marconi, S., Cescatti, A., Quesada, B., Noblet-Ducoudré, N. de, House, J. I., and Arneth, A.: Biophysical effects on temperature and precipitation due to land cover change, Environ. Res. Lett., 12, 053002, https://doi.org/10.1088/1748-9326/aa6b3f, 2017.

Peters-Lidard, C. D., Blackburn, E., Liang, X., and Wood, E. F.: The Effect of Soil Thermal Conductivity Parameterization on Surface Energy Fluxes and Temperatures, 55, 1209–1224, https://doi.org/10.1175/1520-0469(1998)055<1209:TEOSTC>2.0.CO;2, 1998.

Pitman, A. J., Noblet-Ducoudré, N. de, Cruz, F. T., Davin, E. L., Bonan, G. B., Brovkin, V., Claussen, M., Delire, C., Ganzeveld, L., Gayler, V., Hurk, B. J. J. M. van den, Lawrence, P. J., Molen, M. K. van der, Müller, C., Reick, C. H., Seneviratne, S. I., Strengers, B. J., and Voldoire, A.: Uncertainties in climate responses to past land cover change: First results from the LUCID intercomparison study, 36, https://doi.org/10.1029/2009GL039076, 2009.

Prein, A. F., Langhans, W., Fosser, G., Ferrone, A., Ban, N., Goergen, K., Keller, M., Tölle, M., Gutjahr, O., Feser, F., Brisson, E., Kollet, S., Schmidli, J., van Lipzig, N. P. M., and Leung, R.: A review on regional convection-permitting climate modeling: Demonstrations, prospects, and challenges, 53, 323–361, https://doi.org/10.1002/2014RG000475, 2015.

Rechid, D., Davin, E., de Noblet-Ducoudré, N., and Katragkou, E.: CORDEX Flagship Pilot Study "LUCAS - Land Use & Climate Across Scales" - a new initiative on coordinated regional land use change and climate experiments for Europe, 1, n.d.

Ren, Z., Li, Z., Liu, X., Li, P., Cheng, S., and Xu, G.: Comparing watershed afforestation and natural revegetation impacts on soil moisture in the semiarid Loess Plateau of China, 8, 2972, https://doi.org/10.1038/s41598-018-21362-5, 2018.

Rummukainen, M.: Added value in regional climate modeling, 7, 145–159, https://doi.org/10.1002/wcc.378, 2016.

Schrodin, R. and Heise, E.: COSMO Technical Report No. 2: The Multi-Layer Version of theDWD Soil Model TERRA_LM, https://doi.org/10.5676/DWD_PUB/NWV/COSMO-TR_2, 2001.

Semmler, T.: Der Wasser- und Energiehaushalt der arktischen Atmosphäre. PhD thesis, Max Planck Institute for Meteorology, Examensarbeit Nr. 85, 106 pp., 2002.

Skamarock, W., Klemp, J., Dudhia, J., Gill, D., Barker, D., Wang, W., Huang, X.-Y., and Duda, M.: A Description of the Advanced Research WRF Version 3, UCAR/NCAR, https://doi.org/10.5065/D68S4MVH, 2008.

Soares, P. M. M., Cardoso, R. M., Miranda, P. M. A., de Medeiros, J., Belo-Pereira, M., and Espirito-Santo, F.: WRF high resolution dynamical downscaling of ERA-Interim for Portugal, Clim Dyn, 39, 2497–2522, https://doi.org/10.1007/s00382-012-1315-2, 2012.

Strandberg, G. and Kjellström, E.: Climate Impacts from Afforestation and Deforestation in Europe, 23, 1–27, https://doi.org/10.1175/EI-D-17-0033.1, 2019.

Swann, A. L. S., Fung, I. Y., and Chiang, J. C. H.: Mid-latitude afforestation shifts general circulation and tropical precipitation, Proceedings of the National Academy of Sciences, 109, 712–716, https://doi.org/10.1073/pnas.1116706108, 2012.

Swenson, S. C., Burns, S. P., and Lawrence, D. M.: The Impact of Biomass Heat Storage on the Canopy Energy Balance and Atmospheric Stability in the Community Land Model, 11, 83–98, https://doi.org/10.1029/2018MS001476, 2019.

Tölle, M. H. and Churiulin, E.: Sensitivity of Convection-Permitting Regional Climate Simulations to Changes in Land Cover Input Data: Role of Land Surface Characteristics for Temperature and Climate Extremes, 9, 954, https://doi.org/10.3389/feart.2021.722244, 2021.

Tölle, M. H., Engler, S., and Panitz, H.-J.: Impact of Abrupt Land Cover Changes by Tropical Deforestation on Southeast Asian Climate and Agriculture, 30, 2587–2600, https://doi.org/10.1175/JCLI-D-16-0131.1, 2017.

Tölle, M. H., Breil, M., Radtke, K., and Panitz, H.-J.: Sensitivity of European Temperature to Albedo Parameterization in the Regional Climate Model COSMO-CLM Linked to Extreme Land Use Changes, Front. Environ. Sci., 6, https://doi.org/10.3389/fenvs.2018.00123, 2018.

de Vries, D. A.: Thermal Properties of Soils. In: W.R. van Wijk (editor) Physics of the Plant Environment., 1963.

Warrach-Sagi, K., Schwitalla, T., Wulfmeyer, V., and Bauer, H.-S.: Evaluation of a climate simulation in Europe based on the WRF–NOAH model system: precipitation in Germany, Clim Dyn, 41, 755–774, https://doi.org/10.1007/s00382-013-1727-7, 2013.

Wilhelm, C., Rechid, D., and Jacob, D.: Interactive coupling of regional atmosphere with biosphere in the new generation regional climate system model REMO-iMOVE, Geosci. Model Dev., 7, 1093–1114, https://doi.org/10.5194/gmd-7-1093-2014, 2014.

Zhang, S., Yang, D., Yang, Y., Piao, S., Yang, H., Lei, H., and Fu, B.: Excessive Afforestation and Soil Drying on China's Loess Plateau, 123, 923–935, https://doi.org/10.1002/2017JG004038, 2018.

Table 1: Characteristics of the RCMs participating in the study. JLU – Justus-Liebig-Universität Gießen; BTU: Brandenburgische Technische Universität; KIT – Karlsruhe Institute of Technology; ETH – Eidgenössische Technische Hochschule Zürich; SMHI – Swedish Meteorological and Hydrological Institute; ICTP – International Centre for Theoretical Physics; GERICS – Climate Service Center Germany; IDL – Instituto Amaro Da Costa; UHOH – University of Hohenheim; BCCR – Bjerknes Center for Climate Research; AUTH –Aristotle University of Thessaloniki. The full table including the parameterization schemes and settings used, can be found in Davin et al., 2020 and in Table S1 in the supplementary material.

Model label	Institute	RCM version	LSM	Soil column
CCLM-TERRA	JLU/BTU/CMCC	COSMO_5.0_clm9	TERRA-ML (Schrodin and Heise, 2001)	10 layers down to 15.3 m. First 9 (8) layers are thermally (hydrologically) active. The computation of soil thermal conductivity and heat capacity is described in ~~(~~Doms et al., 2013~~)(Doms, 2013) (Doms et al., n.d.)~~
CCLM-VEG3D	KIT	COSMO_5.0_clm9	VEG3D (Breil et al., 2018)	10 layers down to 15 m. First 9 (8) layers are thermally (hydrologically) active. Soil thermal conductivity is based on ~~(~~Johansen, 1977~~)(Johansen, 1977)~~ and the heat capacity on ~~(~~de Vries, 1963~~).~~
CCLM-CLM4.5	ETH	COSMO_5.0_clm9	CLM4.5 (Oleson et al., 2013)	15 thermally active layers down to 42 m. The first 10 layers are hydrologically active. Soil thermal conductivity is computed according to Farouki (1981). Volumetric heat capacity is computed according to ~~(~~de Vries, 1963~~).~~
CCLM-CLM5.0	ETH	COSMO_5.0_clm9	CLM5.0 (Lawrence et al., 2019)	25 thermally active layers down to 50 m. The first 20 layers are hydrologically active. Soil thermal conductivity is computed according to Farouki (1981). Volumetric heat capacity is computed according to ~~(~~de Vries, 1963~~).~~
RegCM-CLM4.5	ICTP	RegCM4.6.1	CLM4.5 (Oleson et al., 2013)	15 thermally active layers down to 42 m. The first 10 layers are hydrologically active. Soil thermal conductivity is computed according to Farouki (1981). Volumetric heat capacity is computed according to ~~(~~de Vries, 1963~~).~~
REMO-iMOVE	GERICS	REMO2009	iMOVE (Wilhelm et al., 2014)	5 thermally active layers down to 9.8 m. One water bucket. The dependency of thermal conductivity and heat capacity on soil moisture is modelled according to ~~(~~Semmler, 2002~~).~~

Formatted: Caption, Keep with next

Formatted Table

Formatted: Font color: Light Blue

Formatted: Font color: Light Blue

WRFa-NoahMP	IDL	WRF381	NoahMP	4 layers down to 2 m. The total heat capacity and thermal conductivity of the mineral soil are computed as proposed by ~~(~~Peters-Lidard et al., 1998~~)~~ ~~(Peters-Lidard et al., 1998)(Peters-Lidard et al., 1998)~~
WRFb-NoahMP	UHOH	WRF381	NoahMP	4 layers down to 2 m. The total heat capacity and thermal conductivity of the mineral soil are computed as proposed by ~~(~~Peters-Lidard et al., 1998~~)~~ ~~(Peters-Lidard et al., 1998)~~
WRFc-NoahMP	BCCR	WRF381	NoahMP	4 layers down to 2 m. The total heat capacity and thermal conductivity of the mineral soil are computed as proposed by ~~(~~Peters-Lidard et al., 1998~~)~~ ~~(Peters-Lidard et al., 1998)~~
WRFb-CLM4.0	AUTH	WRF381	CLM4.0 (Oleson et al., 2010)	10 thermally and hydrologically active layers down to 3.43 m. Soil thermal conductivity is computed according to ~~(~~Farouki~~,~~ (1981)~~)~~. Volumetric heat capacity is computed according to ~~(~~de Vries, 1963~~)~~.

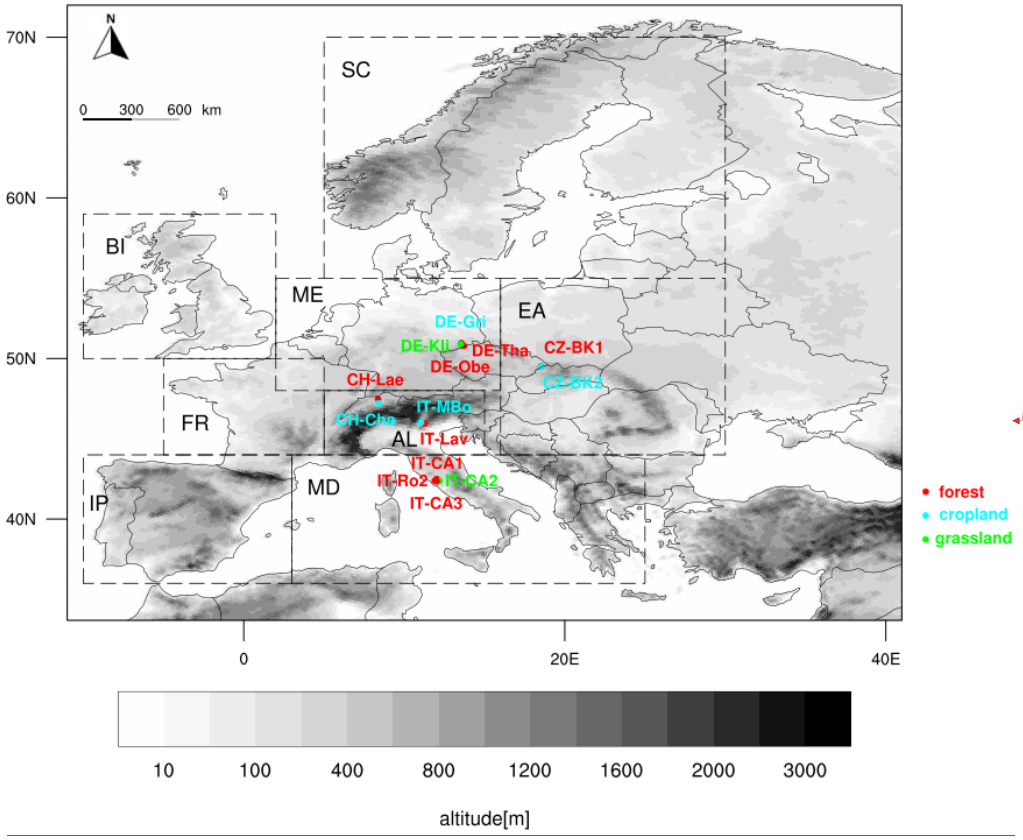

Figure 1: Topography of the model domain and location of the observational pairs. The outlined boxes with a dashed line correspond to the eight regions on which our analysis has been focused: AL (Alps), BI (British Isles), EA (Eastern Europe), FR (France), IP (Iberian Peninsula), MD (Mediterranean), ME (Mid-Europe), SC (Scandinavia).

Formatted: Keep with next

Formatted: Caption

Formatted: Caption, Keep with next

Table 2: Characteristics of the sites selected from FLUXNET2015 dataset. DBF – Deciduous Broadleaf Forest; ENF – Evergreen Needleleaf Forest; MF – Mixed Forest; CRO – cropland; GRA – grassland, as described by the International Geosphere-Biosphere Programme (IGBP) classification scheme.

Pair ID	FLUXNET site ID	(Latitude, Longitude)	Elevation (m)	Land cover type	Distance (km)	Time period	Measurement depth
1	IT-CA1	(42.380,12.026)	200	DBF	0.3	2011-2014	15cm
	IT-CA2	(42.377,12.026)	200	CRO			
2	IT-CA3	(42.380,12.022)	197	DBF	0.4	2011-2014	15cm
	IT-CA2	(42.377,12.026)	200	CRO			
3	IT-Ro2	(42.390,11.920)	160	DBF	8.7	2011-2012	15cm
	IT-CA2	(42.377,12.026)	200	CRO			
4	CZ-BK1	(49.502,18.536)	875	ENF	0.9	2004-2012	5cm
	CZ-BK2	(49.494,18.542)	855	GRA			
5	DE-Tha	(50.962,13.565)	385	ENF	4.1	2004-2014	10cm
	DE-Gri	(50.950,13.512)	385	GRA			
6	DE-Obe	(50.786,13.721)	734	ENF	23.4	2008-2014	10cm
	DE-Gri	(50.950,13.512)	385	GRA			
7	DE-Tha	(50.962,13.565)	385	ENF	8.4	2004-2014	10cm
	DE-Kli	(50.893,13.522)	478	CRO			
8	DE-Obe	(50.786,13.721)	734	ENF	18.4	2008-2014	10cm
	DE-Kli	(50.893,13.522)	478	CRO			
9	IT-Lav	(45.956,11.281)	1353	ENF	19.3	2003-2013	10cm
	IT-Mbo	(46.014,11.045)	1550	GRA			
10	CH-Lae	(47.478,8.364)	689	MF	30	2005-2014	10cm
	CH-Cha	(47.210,8.41)	393	GRA			

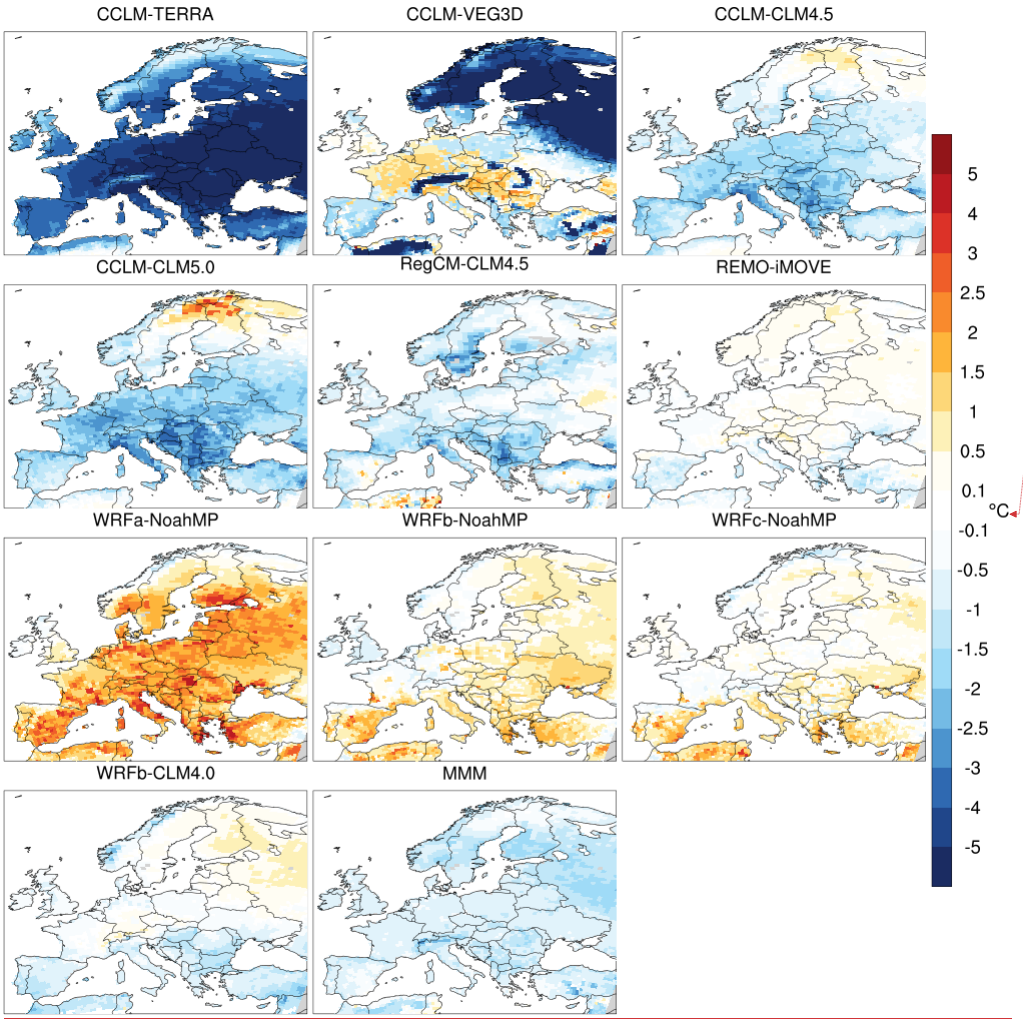

Figure 2: Afforestation (FOREST minus GRASS) impact on the annual amplitude of soil temperature (AAST) at 1 meter depth. MMM: Multi-Model-Mean.

Formatted: Keep with next

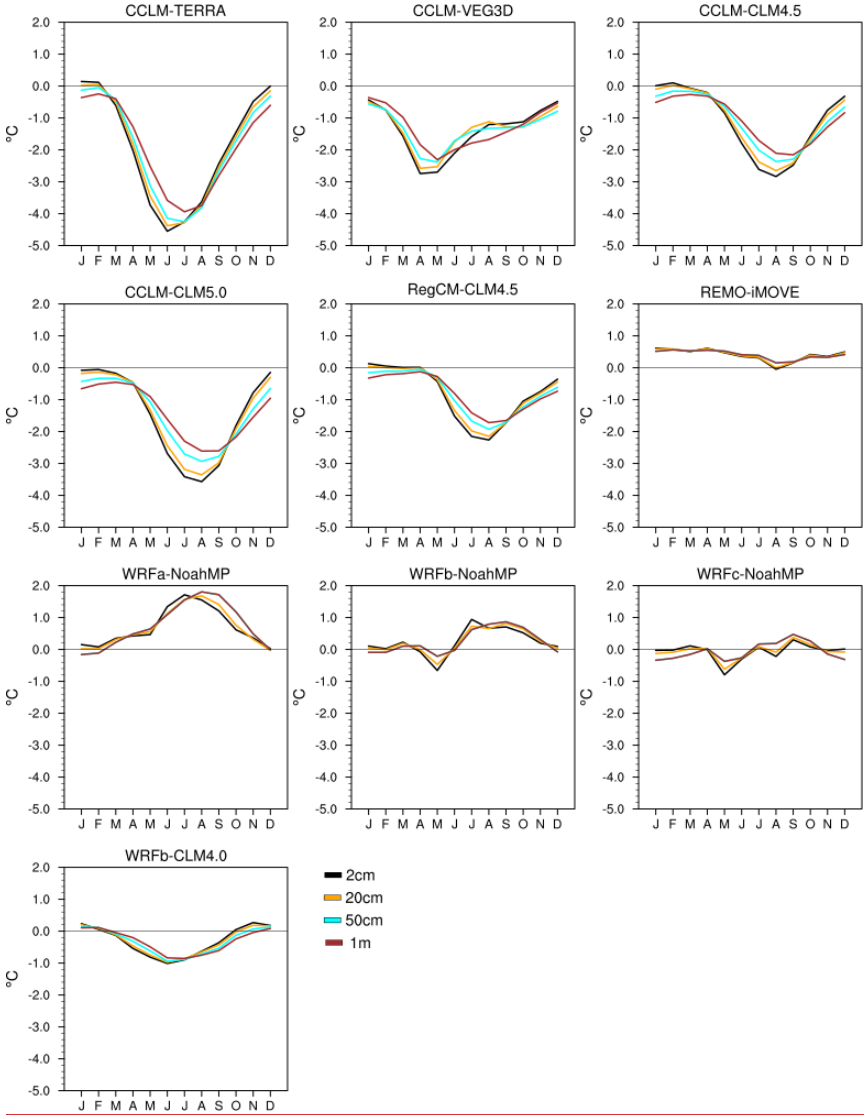

Figure 3: Afforestation impact (FOREST minus GRASS) on mean monthly soil temperature at four different soil depths over Mediterranean.

Formatted: Keep with next

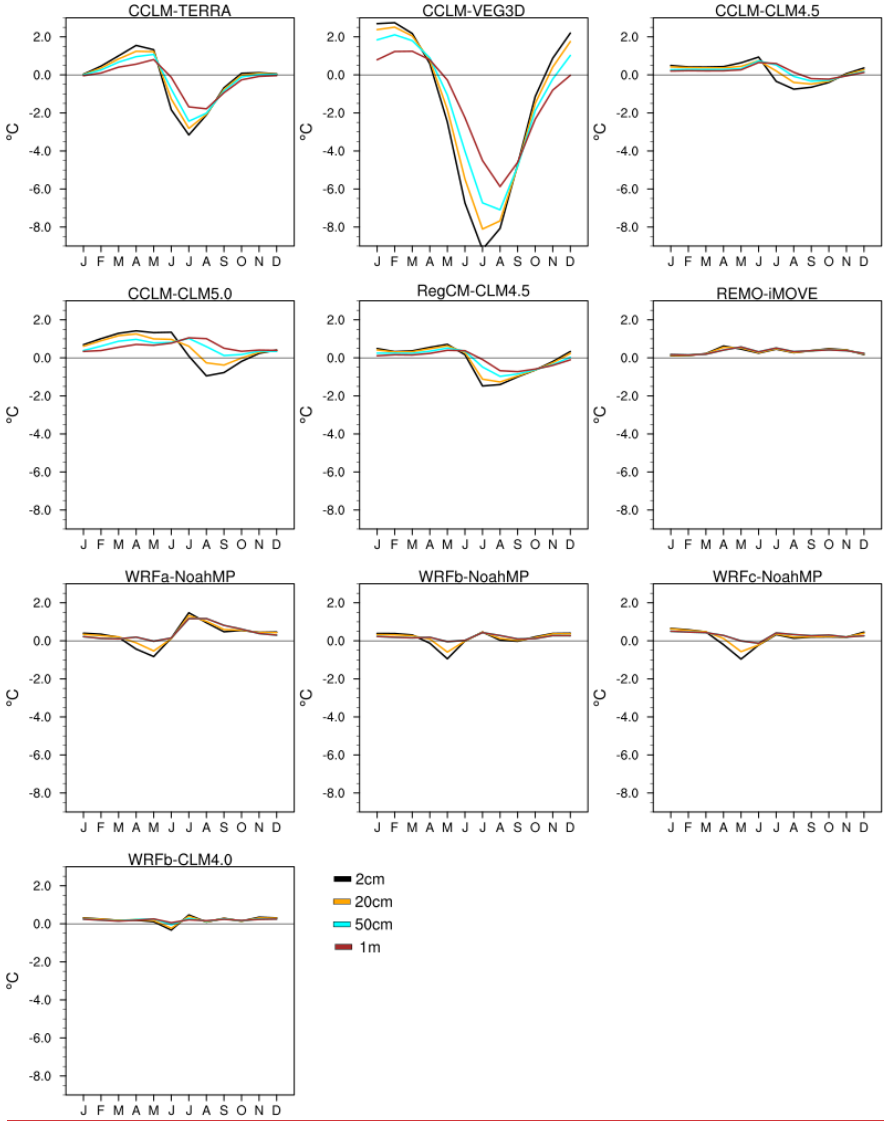

Figure 4: Afforestation impact (FOREST minus GRASS) on mean monthly soil temperature at four different soil depths over Scandinavia.

Formatted: Keep with next

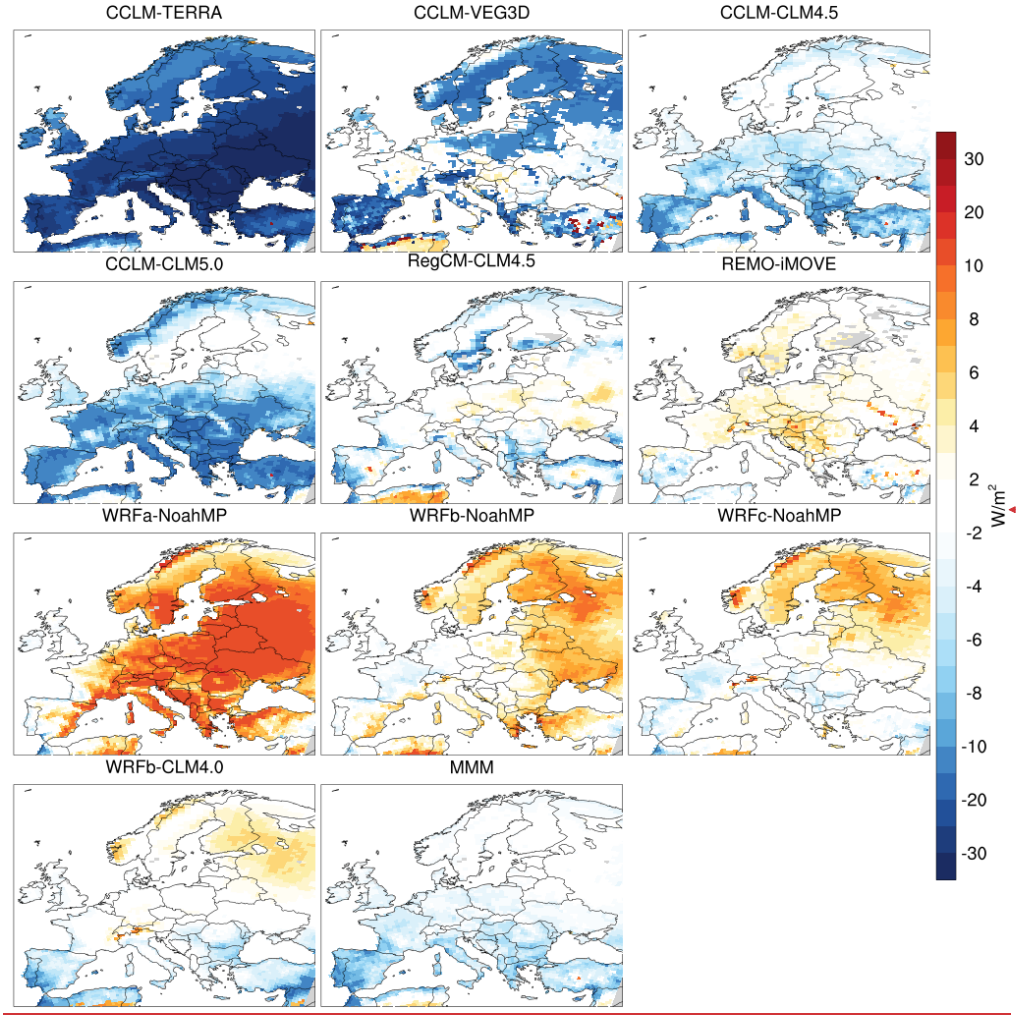

Figure 5: Afforestation impact (FOREST minus GRASS) on the surface energy input into the ground (W/m^{-2}) during summer. Positive (negative) values mean increase (decrease) with afforestation.

Formatted: Keep with next

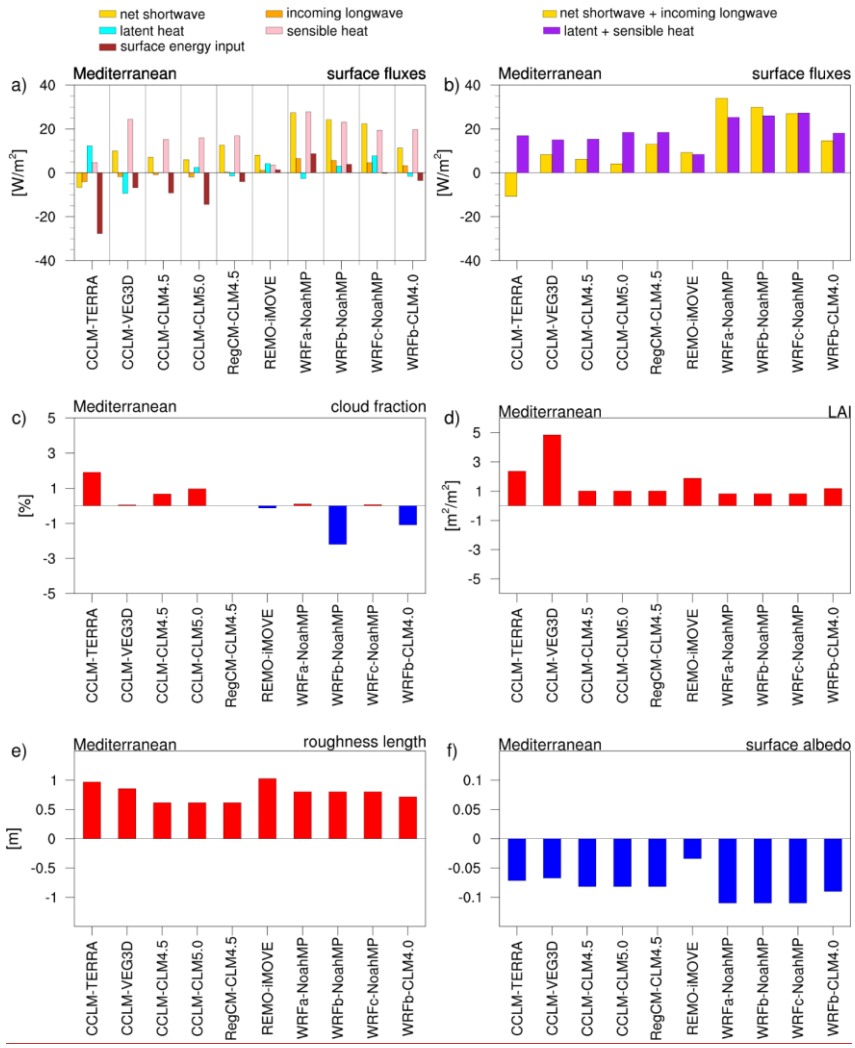

Figure 6: (a) Changes in surface energy balance components (FOREST minus GRASS) averaged over Mediterranean in summer, (b) The changes in available radiative energy at the surface and in the sum of turbulent heat fluxes with afforestation (FOREST minus GRASS), (c) Cloud fraction response to afforestation across models, and the inter-model differences in leaf area index (LAI) (d), surface roughness (e) and surface albedo (f) in summer (yearly maximum). Positive (negative) values mean increase (decrease) with afforestation.

Formatted: Keep with next

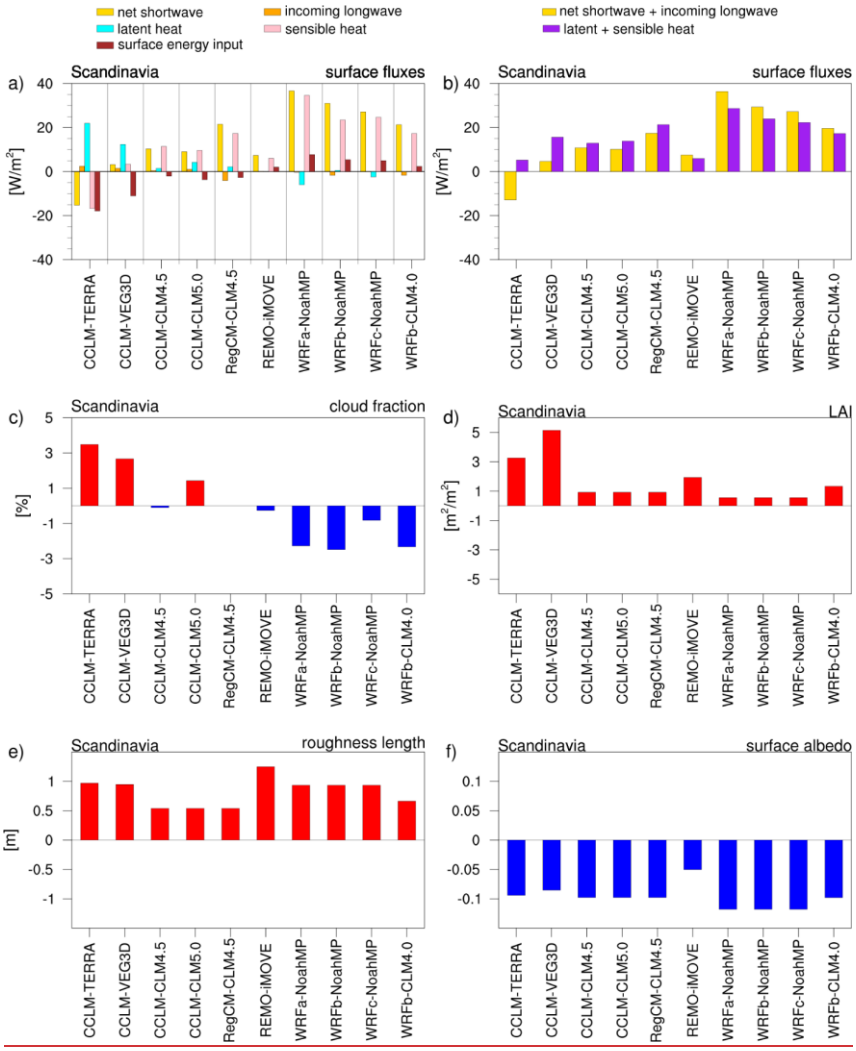

Figure 7: (a) Changes in surface energy balance components (FOREST minus GRASS) averaged over Scandinavia in summer, (b) The changes in available radiative energy at the surface and the sum of turbulent heat fluxes with afforestation (FOREST minus GRASS), (c) Cloud fraction response to afforestation across models, and the inter-model differences in leaf area index (LAI) (d), surface roughness (e) and surface albedo (f) in summer (yearly maximum). Positive (negative) values mean increase (decrease) with afforestation.

Formatted: Keep with next

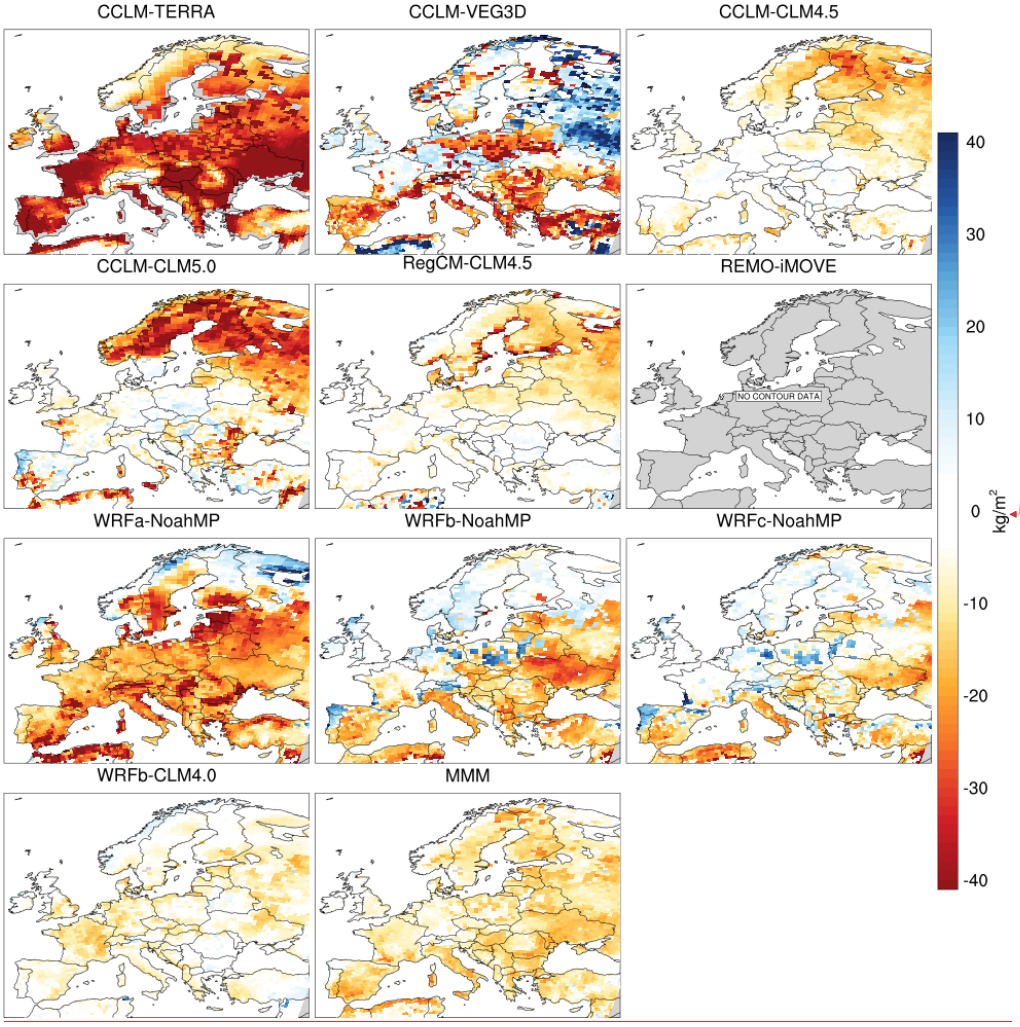

Formatted: Keep with next

Figure 8: Afforestation (FOREST minus GRASS) impact on soil moisture content (kg m^{-2}) of the top 1 meter of the soil during summer. REMO-iMOVE is not included because it employed a bucket scheme for soil hydrology in the LUCAS Phase 1 experiments, which does not allow a separation of soil moisture into different layers.

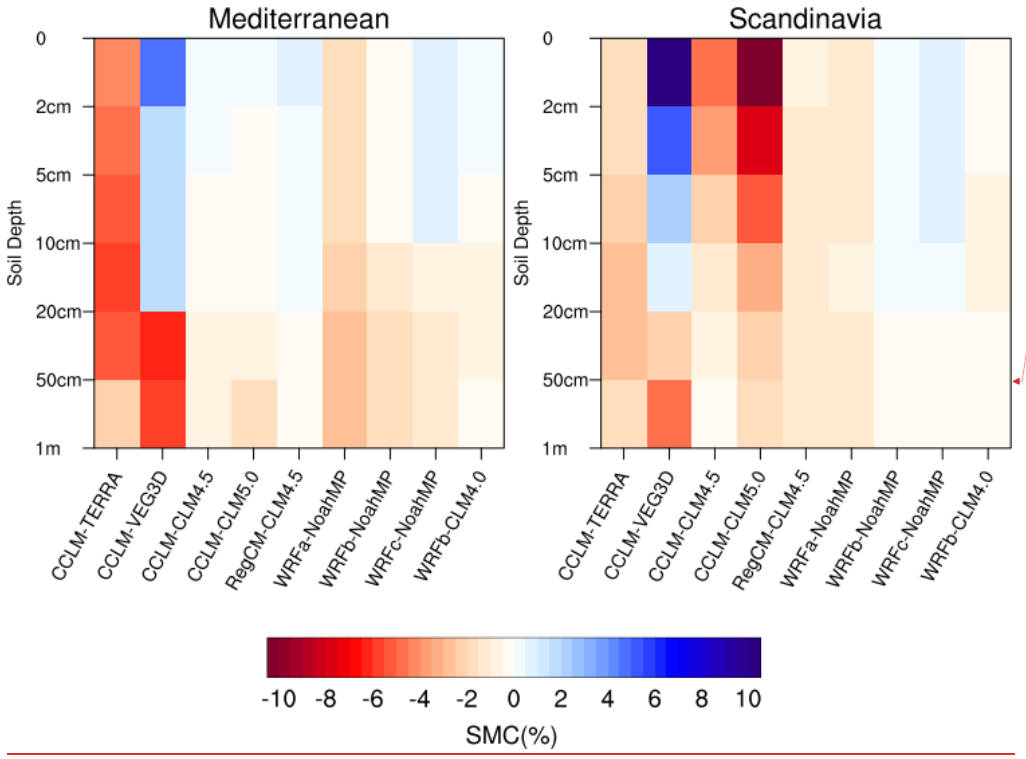

Figure 9: Mean summer changes in soil moisture content (SMC) due to afforestation (FOREST minus GRASS) in the top 1 meter of the soil over Mediterranean and Scandinavia. Positive (negative) values mean an increase (decrease) due to afforestation.

Formatted: Keep with next

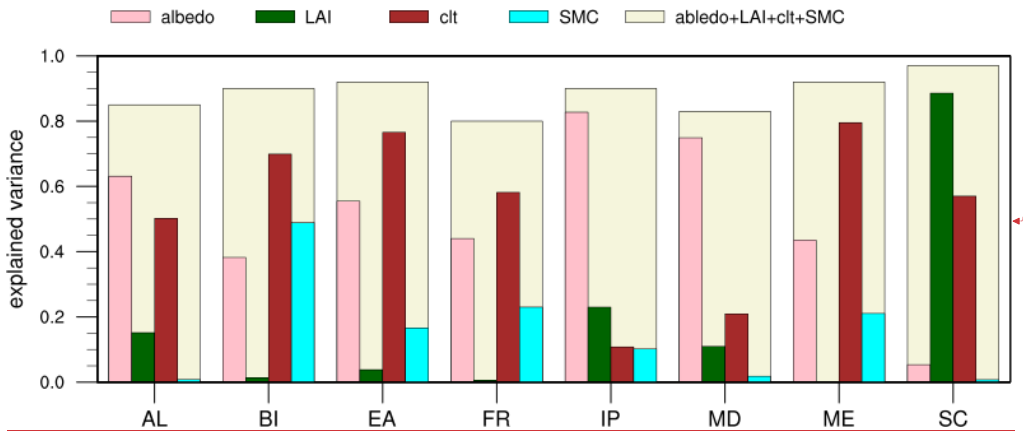

Figure 10: The fraction of inter-model variance in AAST response (FOREST minus GRASS) explained by mean summer changes in albedo, leaf area index (LAI), cloud fraction (clt), soil moisture content (SMC) or all combined (albedo+LAI+clt+SMC). Bars represent the coefficient of determination (R^2) values derived from linear regression analysis applied over each sub-region. Alps (AL), British Isles (BI), Eastern Europe (EA), France (FR), Iberian Peninsula (IP), Mediterranean (MD), Mid-Europe (ME), Scandinavia (SC).

Formatted: Keep with next

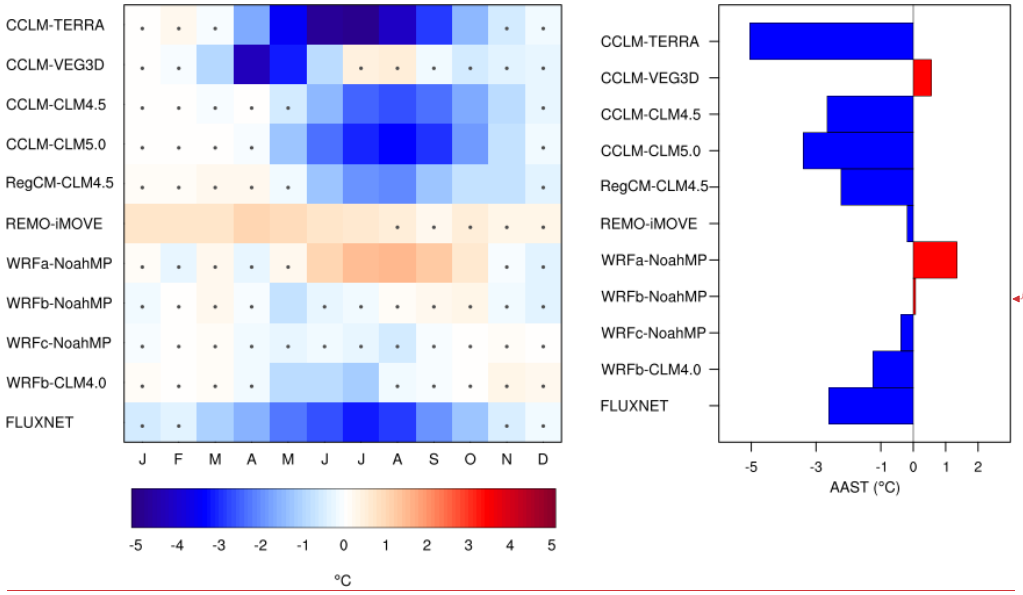

Figure 11: Left: Observed and simulated impact of afforestation on mean monthly soil temperature. The dots indicate the differences which are insignificantly different from zero in a two-sided t-test at 95% confidence level. Right: The changes in AAST (ºC) due to afforestation across models and observations. The observational differences are averaged over all the paired FLUXNET sites (forest minus open land) and the simulated changes are averaged over the corresponding model grids (FOREST minus GRASS). Positive (negative) values mean an increase (decrease) with afforestation.

Formatted: Keep with next

Formatted: Caption